Synthesis of Zinc Oxide Nanoparticles Using Leaf Extract of *Coriandrum sativum* (Dimbilal) and its Application for Antimicrobial and Antioxidant Activity

Birhanesh Kolcha Wodajo

A Thesis Submitted to the Department of Applied Chemistry

School of Applied Natural Science

Presented in Partial Fulfillment of the Requirement for the Degree of Master's in Chemistry (Industrial Chemistry)

Office of Graduate Studies

Adama Science and Technology University

November, 2022

Adama, Ethiopia

Synthesis of Zinc Oxide Nanoparticles Using Leaf Extract of *Coriandrum sativum* (Dimbilal) and its Application for Antimicrobial and Antioxidant Activity

Birhanesh Kolcha Wodajo

Advisor: Fedlu Kedir Sabir (PhD.)

A Thesis Submitted to Department of Applied Chemistry

School of Applied Natural Science

Presented in Partial Fulfillment of the Requirement for the Degree of Master's in Chemistry (Industrial Chemistry)

Office of Graduate Studies

Adama Science and Technology University

November, 2022

Adama, Ethiopia

DECLARATION

I hereby declare that this Master Thesis entitled "**Synthesis of Zinc Oxide Nanoparticles Using Leaf Extract of *Coriandrum sativum* (Dimbilal) and its Application for Antimicrobial and Antioxidant Activity**" is my original work. It has not been submitted for the award of any academic degree, diploma or certificate in any other university. All sources of materials that are used for this thesis have been duly acknowledged through citation.

Birhanesh Kolcha Wodajo _____ _____

Name of the student Signature Date

RECOMMENDATION

I, the advisor of this thesis, hereby certify that I have read the revised version of the thesis entitled "**Synthesis of Zinc Oxide Nanoparticles Using Leaf Extract of *Coriandrum sativum* (Dimbilal) and its Application for Antimicrobial and Antioxidant Activity**" prepared under my guidance by Birhanesh Kolcha Wodajo submitted in partial fulfillment of the requirements for the degree of Mater's of Science in Industrial Chemistry. Therefore, I recommend the submission of revised version of the thesis to the department following the applicable procedures.

Fedlu Kedir Sabir (PhD.) _____ _____

Major Advisor Signature Date

APPROVAL PAGE

I, the advisor of this thesis, hereby certify that I have read the revised version of the thesis entitled "**Synthesis of Zinc Oxide Nanoparticles Using Leaf Extract of *Coriandrum sativum* (Dimbilal) and its Application for Antimicrobial and Antioxidant Activity**" developed by Birhanesh Kolcha; hereby certify that the recommendation and suggestion made by the board of examiners are appropriately incorporated into the final version of the thesis.

Dr. Fedlu Kedir _____ _____

Major Advisor Signature Date

We, the undersigned, members of the Board of Examiners of the thesis by Birhanesh Kolcha have read and evaluated the thesis entitled "**Synthesis of Zinc Oxide Nanoparticles Using Leaf Extract of *Coriandrum sativum* (Dimbilal) and its Application for Antimicrobial and Antioxidant Activity**" and examined the candidate during open defense. We certify that the thesis is accepted for partial fulfillment of the requirement of the degree of Master of Science in Industrial Chemistry.

Dr. Akalu Terefa _____ _____

Chairperson Signature Date

Dr. Bayisa Meka _____ _____

Internal Examiner Signature Date

Prof. Sisay Tadesse _____ _____

External Examiner Signature Date

Final approval and acceptance of the thesis is contingent upon submission of its final copy to the Office of Postgraduate Studies through the Department Graduate committee and School Graduate Committee.

_____ _____ _____

Department Head Signature Date

_____ _____ _____

School Dean Signature Date

_____ _____ _____

Office of Postgraduate Studies, Dean Signature Date

ACKNOWLEDGEMENT

First, I give all glory and honor to God, the source of all wisdom, knowledge, understanding, health, and strength. Then I would like to give my honorable thanks to the Chemical and Construction Input Industry Research and Development Center, particularly for giving me this chance to study at Adama Science and Technology University (ASTU). And foremost, the completion of this research work would not have been possible without the excellent guidance of my advisor, Dr. Fedlu Kedir (PhD.). I acknowledge all his encouragement and valuable time given to me with deep gratitude and appreciation.

I would also like to acknowledge all the academic staff members and laboratory assistants of Department of Applied Chemistry at ASTU.

Finally, I must express my very profound gratitude to all my staff members (Eden, Elsabet, Meki, Desta, Yibeltal, Misa, Alemayehu, Mesfin, Betsilase, and Eskinder), my friends (Dr. Yetemwork Zawga, Tigist Abate, Abate Kasaw, Cherenet Ahamed, Oliqa Mamo, Keneni Debelu, Fasika Dereje, Ilile Dine, Iman Mustefa) and my parents (Somome Musa, Siraj Abdu with his family, Aregash Abdu with her family, Ashenafi Abdu with his family and Mebirat Kolcha) for providing me with unfailing support and continuous encouragement throughout my years of study and through the process of researching and writing this thesis. This accomplishment would not have been possible without them. Thank you.

TABLE OF CONTENTS

DECLARATION i

RECOMMENDATION ii

APPROVAL PAGE iii

ACKNOWLEDGEMENT iv

LIST OF TABLES viii

LIST OF FIGURES ix

LIST OF ABBREVIATIONS x

ABSTRACT xi

CHAPTER ONE 1

1. INTRODUCTION 1

1.1. Background of the Study 1

1.2. Statement of the Problems 3

1.3. Objectives of the Study 4

1.3.1. General objective 4

1.3.2. Specific objectives 4

1.4. Significance of the Study 5

1.5. Scope of the Study 5

CHAPTER TWO 6

2. LITERATURE REVIEW 6

2.1. Introduction to Nanotechnology and Nanoparticles 6

2.1.1. Classification of nanoparticles 7

2.2. Zinc Oxide Nanoparticles 10

2.2.1. Properties of ZnO nanoparticle 11

2.3. Synthesis Methods of Zinc Oxide Nanoparticles 13

2.3.1. Physical method 15
2.3.2. Chemical method 15
2.3.3. Green synthesis method 16
2.4. Characterization Technique 17
2.5. Application of ZnO NPs 17
2.5.1. Antimicrobial activity 18
2.5.2. Antioxidant activity of ZnO NPs 19
2.5.3. Photocatalytic activity of ZnO NPs 20
2.5.4. Application of ZnO NPs in cosmetics 21
2.5.5. Biomedical application of ZnO NPs 22
2.5.6. Agricultural applications of ZnO NPs 22
2.6. *Coriandrum sativum* (Dimbilal) 23
2.6.1. The composition of *Coriandrum sativum* 24
CHAPTER THREE 25
3. MATERIALS AND METHODS 25
3.1. Study Site Description 25
3.2. Chemicals and Reagents 25
3.3. Materials and Instruments 25
3.4. Methods 26
3.4.1. Preparation of *Coriandrum sativum* leaf extract 26
3.4.2. Phytochemical screening of *Coriandrum sativum* plant leaf extract 27
3.4.3. Green synthesis of ZnO nanoparticles 28
3.4.4. Characterization of ZnO nanoparticles 29
3.4.5 Antibacterial activity 30
3.4.6. Antifungal activity 31

3.4.7. Antioxidant activity 32
CHAPTER FOUR 33
4. RESULTS AND DISCUSSION 33
4.1. Phytochemical Screening of *Coriandrum sativum* leaf Extract. 33
4.2. Characterization Analysis 35
4.2.1. Thermal Analysis (TGA/DTA) of ZnO NPs 35
4.2.2. X-Ray Diffraction (XRD) of ZnO NPs analysis 36
4.2.3. UV-Vis spectrophotometric analysis of ZnO NPs 41
4.2.4. Fourier Transforms Infrared Spectroscopy (FTIR) analysis 43
4.2.5. Scanning Electron Microscopy (SEM) analysis 45
4.3. Antimicrobial Activity Test of ZnO NPs 47
4.3.1. Antibacterial activity test of ZnO NPs 47
4.3.2. Antifungal activities of ZnO NPs 51
4.3.3. Antioxidant activities of ZnO NPs 54
5. CONCLUSIONS AND RECOMMENDATIONS 58
5.1. Conclusions 58
5.2. Recommendation 58
6. REFERENCE 59

LIST OF TABLES

Table 1 Results of phytochemical screening of aqueous extracts of Coriandrum sativum leaf. .. 34
Table 2 Structural parameters of prepared ZnO nanoparticles. 40
Table 3. The effects of the plant extract on the optical properties and sizes of ZnO NPs. 41
Table 4 Zone of inhibition (mm) of ZnO NPs against gram-positive and gram-negative bacteria pathogens. 50
Table 5. Zone of inhibition of synthesized ZnO NPs on the selected fungal strains 53
Table 6 The percent radical scavenging activity value from the DPPH assay of ZnO NPs ratios and ascorbic acid..... 55

LIST OF FIGURES

Figure 1 The crystal structures (left to right) zinc blende, wurtzite (ZnO), and rocksalt. 12
Figure 2 Different synthesis approaches used in metallic nanoparticles 14
Figure 3 The photo of *Coriandrum sativum* (Dimbilal) plant leaf. 24
Figure 4 Preparation of *Coriandrum sativum* leaf extract. 26
Figure 5 Synthesis of ZnO NPs using green synthesis method. 28
Figure 6 Phytochemical test for aqueous extract *Coriandrum sativum* leaf to steroids (A), glycosides (B), benedict (C), taninns (D), flavonoids (E), phenol (F), alkaloids (G), saponins (H), and terpenoids (I). 34
Figure 7 Thermal analysis of synthesized ZnO NPs (1:1) ratio..... 36
Figure 8 XRD patterns of ZnO nanoparticles synthesized under different ratios of zinc nitrate salt and Coriandrum sativum leaf extract. 38
Figure 9 UV-Vis absorption spectra (A) for ZnO NPs synthesized by different ratios of plant extract to precursor solution..... 42
Figure 10 The energy band gap determination (B) for ZnO NPs synthesized by different ratios of plant extracts to precursor solution. 43
Figure 11 FT-IR spectrum for ZnO NPs calcined A (CZnO), uncalcined ZnO NPs B (UCZnO), and *Coriandrum sativum* leaf extract C (Cs Leaves). 45
Figure 12 SEM images of ZnO NPs A (1:1), B (3:2), and C (2:3) ratios. 47
Figure 13 Antibacterial activity of synthesized ZnO NPs against bacterial pathogens, A, B, and C represent 50, 75, and 100 µg/mL respectively. 49
Figure 14 Antifungal activity of Synthesized ZnO NPs against selected fungal strains BK-11, BK-23, BK-32, AN, and C.A represents ZnO NPs 1:1, 2:3, and 3:2 ratios, *Aspergillus niger* and *Candida albicans* respectively. 53
Figure 15 In the DPPH assay of ZnO NPs ratios and ascorbic acid concentration versus absorbance graph. 56
Figure 16 DPPH assay of the synthesized ZnO NPs antioxidant activity at 50, 100, 200, 400, and 800 µg /mL concentration. 56

LIST OF ABBREVIATIONS

ASTU	Adama Science and Technology University
CSLE	*Coriandrum Sativum* Leaves Extract
CNT	Carbon Nano Tubes
CZnO NPs	Calcinated Zinc Oxide Nanoparticles
DH_2O	Distilled water
DMSO	Dimethyl Sulfoxide
DPPH	2, 2- diphenyl-1-picryl hydroxyl
FT-IR	Fourier Transform Infrared Spectroscopy
MHA	Mueller Hinton Agar
NPs	Nano Particles
PDA	Potato Dextrose Agar
ROS	Reactive Oxygen Species
RPM	Revolution Per Minute
RSA	Radical Scavenging Activity
SDA	Sabouraud Dextrose Agar
SEM	Scanning Electron Microscopy
TGA-DTA	Thermal Gravimiteric- Differential Thermal Analysis
UCZnO NPs	Uncalcinated Zinc Oxide Nanoparticles
UV-Vis	Ultraviolet-Visible absorption spectroscopy
XRD	X-Ray Diffractions
ZnO NPs	Zinc oxide Nanoparticles

ABSTRACT

Green synthesis of nanoparticles (NPs) using plant extract is a novel method to develop environmentally benign nanomaterials which can be used in numerous biomedical applications. This work addressed a low-cost, non-toxic green synthesis of zinc oxide nanoparticles prepared using different amounts of leaf extract and precursor. This study aimed to synthesize ZnO NPs using Coriandrum sativum leaf extract through a green synthesis approach and apply for antimicrobial and antioxidant activity. The synthesized nanoparticles were characterized using Thermal Gravimetric- Differential Thermal Analysis (TGA-DTA), X-Ray diffraction (XRD), Fourier transform infrared (FTIR) spectroscopy, Ultraviolet-Visible absorption spectroscopy (UV-Vis), and Scanning Electron Microscopy (SEM). The average crystal size of the synthesized NPs was calculated using the Debye Scherer equation. The average crystal size of ZnO NP was found to be 13.85nm (3:2 ratio), 15.850nm (1:1), 17.91nm (2:3) uncalcinated, and 19.29nm (1:1) calcinated ZnO NPs for green synthesis method. The XRD pattern with sharp peaks describes the crystalline and purity of zinc oxide nanoparticles. The FTIR spectrum of zinc oxide (Zn-O) nanoparticles absorbs at 660 cm^{-1} and 818 cm^{-1} for both calcined and uncalcinated respectively. FTIR spectrum showed the interaction between the functional groups of the phytochemical in the Coriandrum sativum leaves extract and the ZnO NPs. Antibacterial activity of 3:2 ZnO NPs ratio in 100 µg/mL concentration ranges showed a greater zone of inhibition 12 mm against Gram positive (Staphylococcus aureus) *and Gram negative (Escherichia coli*) *bacterial pathogens compared to other ratios and also 3:2 ZnO NPs showed greater antifungal activity in both Candida albicans and Aspergillus niger strains in all concentration. The antioxidant activity of the 1:1 ratio of ZnO NPs showed better activity in high concentrations of 800 µg/mL and it was good efficacy compared with other ratios as the standard ascorbic acid.*

***Keywords*:** Green synthesis, Zinc Oxide nanoparticles, *Coriandrum sativum*, antimicrobial, and antioxidant activity.

CHAPTER ONE

1. INTRODUCTION

1.1. Background of the Study

An advanced branch of science and technology called nanotechnology is concerned with creating and developing nanomaterials with particle sizes between 1 and 100 nm. The interdisciplinary fields of nanoscience and nanotechnology have the potential to spark the next industrial revolution and have been shown to have positive effects on society and the economy in the twenty-first century (R. Sharma et al., 2020). The study and use of materials at the nanoscale is the subject of the large field of nanoscience. It is gaining popularity steadily. Nanoparticles (NPs) exhibit new and improved properties when compared to their bulk counterparts as a result of changes in their characteristics, such as form size, size distribution, and a clearer understanding of the relationship between surface area and size. Due to their unique electrical, mechanical, optical, and magnetic properties, metal oxide nanoparticles have had a wide range of applications in research and innovation in recent years. Zinc oxide nanoparticles (ZnO NPs) have attracted a great deal of interest from researchers in recent years due to their critical applications as antibacterial agents, photovoltaic cells, textile textiles, and polymers to destroy microbes (Degefa et al., 2021).

Because they are eco-friendly, biocompatible, secure, and economical, green syntheses have a significant impact. Plants, bacteria, algae, fungi, and other organisms that are at the base of synthesis can use this technique to produce more with fewer contaminants. Plant extract contains phytochemicals that function as stabilizing and reducing agents. These plant components, such as leaves, seeds, stems, and fruits have been employed as fuel to create ZnO nanoparticles (Ranganatha et al., 2019).

The most significant and varied applications of zinc oxide nanoparticles (ZnO NPs) are photocatalysis, antimicrobial defense, and water purification. Different characteristics distinguish ZnO NPs from regular zinc oxide particles. ZnO NPs have a large band gap (3.37 eV), which enables them to effectively produce electron-holes when UV radiation strikes their surface, allowing them to be used as photocatalysts for the degradation of textile waste and the removal of

industrial heavy metal ions as well as in electronic devices. Additionally, they are utilized in the cosmetic industry to create sunscreen creams that shield the human body from UV rays. Specific biological applications choose ZnO NPs due to their desired characteristics, including their non-toxicity and biocompatibility (R. Sharma et al., 2020)

An annual herb used as a spice, *Coriandrum sativum* (Dimbilal) leaf is a member of the Umbelliferae/Apiaceae family. It is utilized as a spice in the food, beverage, pharmaceutical, fragrance, and medical fields. There are several regional names for it in Ethiopia, including dembilal (Amharic), Debo, shucar (Afanoromo), Tsagha, Zagda (Tigrignya), and Tibichota (Konsonya). To make "Data," a traditional spice used as a Wot with meat and fish, the leaves and immature fruits are utilized as a component. Due to the mild sweet test of the essential oil, it can be used as a starting material in many products, the fatty oil is used as an ingredient for the manufacturing of high-grade engineering plastics (Kassahun, 2018).

Infectious diseases make up a sizable component of the health issues in underdeveloped nations. Since their invention, antibiotics have been crucial in the fight against various infectious diseases and have significantly improved human life by lowering morbidity. But over the previous few decades, they brought about a significant clinical issue in the treatment of infectious diseases because of their side effects and the rise of germs that were resistant to antibiotics. Scientists were compelled by this circumstance to investigate newer antimicrobial medications from diverse sources, such as plants, that had fewer adverse effects and showed less resistance (Jameel et al., 2018).

Bacteria and their phages are the oldest and most abundant life forms on the planet. Bacteria have co-evolved with us and are beneficial for human health. Although we also live in an environment replete with bacteria that can cause a wide variety of human diseases with bacterial infections responsible for 25 percent of human deaths globally, a number is predicted to increase dramatically with the growing crisis of antibiotic resistance (Jubeh et al., 2020). Fungi are important environmental creatures that also provide numerous advantages to contemporary society through their use in the pharmaceutical, beverage, and food sectors. Fungal pathogens, on the other hand, are emerging dangers to people, animals, plants, and insects, and they have the power to cause terrible morbidity, mortality, and economic damage (Hernandez & Martinez, 2018). Bacteria can have a huge impact on the industry and national and financial interests. The usefulness of microbial

biomineralization in construction materials has been established in principle in the laboratory and several field trials. However, several challenges still have to be overcome. For example, methods for optimizing the survival of the bacteria within the concrete are currently being developed (Stanaszek-Tomal, 2020).

Due to their ability to induce blood-borne infections and acquire resistance to numerous common antifungal medications, including Amphotericin B and Fluconazole, fungi (*Candida albicans* and *Aspergillus niger*) represent a significant threat to human health. The ubiquitous fungus *Aspergillus* can be found both inside and outside of buildings. Most people inhale Aspergillus spores every day without getting sick. A person with a compromised immune system or lung disease, however, may make them more susceptible to developing aspergillosis. Another genus of fungus, *Candida albicans*, is harmful to humans. Allergies, lung infections, and infections in other organs are included in the disease spectrum. As a result of the prolonged use of these antifungal medications/antibiotics, susceptible candidal species perish while resistant species tend to spread out and pose a major threat to the hosts (Jameel et al., 2018). It has been decided to broaden the selection of antimicrobial medications derived from plant resources.

Free radicals are unfavorable substances that are created naturally by numerous biological processes in our bodies, including respiration, food digestion, alcohol, and drug metabolism, and the conversion of fats to energy. The natural antioxidant mechanism in our bodies normally eliminates free radicals. Free radicals can cause a negative chain reaction in the body if this system is unable to control them. This reaction can destroy cell membranes, obstruct the activity of key enzymes, prevent vital cellular processes, disrupt normal cell division, destroy DNA, and prevent the body from producing energy (Sharifi-Rad et al., 2020). According to reports, oxidative stress is linked to the emergence of several metabolic, long-term conditions, or malignancies. An important part of these defense systems was played by antioxidants. A careful equilibrium between oxidants and antioxidants allows healthy organisms to resist the damaging effects of reactive oxygen species (Sharifi-Rad et al., 2020).

1.2. Statement of the Problems

The use of *Coriandrum sativum* (C. *Sativum*) plant leaf extract in the green production of zinc oxide nanoparticles (ZnO NPs) and their application for antibacterial and antioxidant activity are motivated by a few fundamental issues. The first is the daily rise in microbial infectious diseases

and the rise in bacterial and fungal resistance to previously used antimicrobials; as a result, it is getting harder for communities to choose an effective antimicrobial drug empirically. Bacterial infection diseases are a severe public health issue that has gained international attention as a hazard to human health that also has implications for the economy and society. It is crucial to teach society about the medical benefits of this natural resource because humans rely heavily on nearby natural resources to maintain their health.

Different types of bacteria, fungi, and even plants are used to make various antibacterial and antifungal medications. However, some antibiotics are extremely expensive, and others are hazardous to both people and the environment. To ensure our society's survival and health against numerous diseases, it is necessary to discover the simplest ways for synthesizing affordable and nontoxic medications. In this study work, ZnO NPs will be made from a leaf extract of the *Coriandrum sativum* leaf. Since it uses locally accessible resources, green synthesis is environmentally safe, non-toxic, and cost-effective. Limited scientific report on the antimicrobial and antoxidant activities of ZnO NPs from leaf extract of *Coriandrum sativum*. Therefore, this work was intended to explore these problems to induce further investigations in these areas by addressing new techniques, benefiting from the unique features of zinc oxide nanoparticles synthesized from zinc nitrate precursor salt in the presence of *Coriandrum sativum* leaves extract.

1.3. Objectives of the Study

1.3.1. General objective

The general objective of this study is to synthesize ZnO nanoparticles using *Coriandrum sativum* leaf extract and evaluate its antimicrobial and antioxidant activity.

1.3.2. Specific objectives

- To screen phytochemicals of the aqueous leaf extract of *Coriandrum sativum*,
- To synthesize ZnO nanoparticles using leaf extract of *Coriandrum sativum* and zinc nitrate hexahydrate ($ZnNO_3)_2.6H_2O$) salt.
- To characterize the synthesized ZnO nanoparticles using UV- Visible spectroscopy (UV-Vis), XRD, TGA-DTA, FTIR, and SEM.

- To study the antibacterial and antifungal activities of zinc oxide nanoparticles against two gram-positive, two gram-negative bacteria pathogens and two fungal strains.
- To study antioxidant activities of zinc oxide nanoparticles.

1.4. Significance of the Study

This study gives information for the researchers about synthesis and helps to use ZnO NPs by biosynthesized method for antimicrobial application in a low cost, simple, and environmentally eco-friendly for community and industrial researchers. The green synthesis of nanoparticles from *Coriandrum sativum* leaf for antimicrobial activity is not well known rather than using it as an ingredient for the preparation of ‘‘Data’’, a traditional spice eaten as a Wot together with meat and fish. So this research will show active compounds that are available in the local plant *Coriandrum sativum.* The synthesis of ZnO NPs is also expected to make the protection and or removal of bacterial and fungal microbes easy, and effective this was one of the ways of keeping people healthy.

1.5. Scope of the Study

The scope of this study was limited to the synthesized of ZnO NPs using *C.sativum* leaf extract, Characterizations of the synthesized nanoparticles using, UV-Vis, XRD, TGA-DTA, FT-IR, and SEM, and the evaluation of the antimicrobial and antioxidant activity of the synthesized nanoparticles.

CHAPTER TWO

2. LITERATURE REVIEW

2.1. Introduction to Nanotechnology and Nanoparticles

Nanotechnology is a field of study that encompasses the investigation of nanoscale phenomena. It is a sub classification of technology within the fields of colloidal science, chemistry, physics, biology, and other sciences. Even if the scientific community is fascinated by the topic of nanoscience, it is a mindset to use single atoms and molecules to create functional structures in any nanotechnology that has applications in the real world. It can have a big impact on how innovative methods are expanded to make new products, replace existing production equipment, and reformulate novel materials and chemicals for better performance, which leads to less material and energy consumption, less environmental damage, and environmental remediation. Although reducing matter and energy consumption is good for the environment, nanotechnology offers the exciting prospect of resolving issues in a more environmentally friendly manner (Nasrollahzadeh et al., 2019).

In medicinal chemistry, atomic physics, and all other domains that are now known, nanoparticles that are between one and one hundred nanometers in size are used extensively (Lakshmi et al., 2017). Nobel Prize winner Richard P. Feynman was the first to give a lecture in 1959 that served as the intellectual inspiration for nanotechnology. NPs come in a variety of forms, dimensions, and topologies. They may have an irregular shape, such as spherical, cylindrical, conical, tubular, hollow core, spiral, etc. Atom clusters are typically favoured when NP sizes are less than 1 nm. NPs can have a uniform or uneven surface. Additionally, they can exist as single- or multi-crystal solids in crystalline and amorphous forms. A multi-crystal solid may be agglomerated or loose. These NPs' change in size & shape has a major impact on their physicochemical characteristics. Due to their distinctive physical and chemical characteristics, NPs have had considerable success in a range of applications across numerous industries (Kumari & Sarkar, 2021). Nanoparticles have a complex structure. They are comprised of two or three layers: (i) a surface layer: functionalized by a variety of small molecules, metal ions, surfactants, or polymers (ii) The shell layer: which can be purposely added and is chemically different from the core, and (iii) The core material: the

central portion of NPs. The characteristic properties of NPs are generally due to the core material. Hence, NPs are often referred to by their core material only. (Joudeh & Linke, 2022).

Since ancient times, nanoparticles have been used in ceramics and medicine. There are various excellent processes for creating nanoparticles. Plants create nanoparticles that are more stable and synthesize them at a higher rate than other types of organisms (Xu et al., 2021). (Lakshmi et al., 2017). These technologies for manufacturing nanoparticles have primarily been developed in recent years due to their cost effectiveness and minimal to no maintenance requirements (Ranganatha et al., 2019). Nanoparticles have replaced traditional semiconductor materials in nanoscale devices such nano-generators, gas sensors, highly effective solar cells, field-emission transistors, ultraviolet photodetectors, and medicinal systems because of their superior optical and electrical capabilities (M. R. A. Kumar et al., 2019).

2.1.1. Classification of nanoparticles

Based on their composition, NPs are generally placed into three classes: organic, carbon-based, and inorganic (Joudeh & Linke, 2022), (Ealias & Saravanakumar, 2017).

2.1.1.1. Organic nanoparticles

The terms "organic nanoparticles" or "polymers" are widely used to describe dendrimers, micelles, liposomes, ferritin, etc. According to earlier research by Mahesh Kumar Teli et al. and L. Mazzola, nanoparticles are biodegradable and non-toxic, while some particles, including micelles and liposomes, have a hollow core known as nanocapsules that are sensitive to thermal and electromagnetic radiation, including heat and light (Mazzola, 2003). These unique characteristics make them an ideal choice for drug delivery. The drug-carrying capacity, stability, and delivery systems, either entrapped drug or adsorbed drug system determine their field of applications and their efficiency apart from their normal characteristics such as the size, composition, surface morphology, etc. Organic nanoparticles are most widely used in the biomedical field, for example, in drug delivery systems as they are efficient and also can be injected into specific parts of the body which is also known as targeted drug delivery (Ealias & Saravanakumar, 2017).

These NPs are typically non-toxic, bio-degradable, and can in some cases, e.g., for liposomes, have a hollow core. Organic NPs are sensitive to thermal and electromagnetic radiation such as heat and light. In addition, they are often formed by non-covalent intermolecular interactions, which makes them more labile and offers a route for clearance from the body. Different parameters determine

the potential field of application of organic NPs, e.g., composition, surface morphology, stability, carrying capacity, etc. Today, organic NPs are mostly used in the biomedical field in targeted drug delivery and cancer therapy (Joudeh & Linke, 2022).

2.1.1.2. Carbon-based

The nanoparticles made completely of carbon are known as carbon-based. Previously Anu Mary Ealias and Saravanakumar M. P can be classified into fullerenes, graphene, carbon Nanotubes (CNT), carbon nanofibers, and carbon black and sometimes activated carbon in Nano size and are presented. Fullerenes (C_{60}) are carbon molecule that is spherical and made up of carbon atoms held together by sp_2 hybridization (Ealias & Saravanakumar, 2017). About 28 to 1500 carbon atoms form the spherical structure with diameters up to 8.2 nm for a single layer and 4 to 36 nm for multi-layered fullerenes. Graphene is an allotrope of carbon. Graphene is a hexagonal network of honeycomb lattices made up of carbon atoms on a two-dimensional planar surface. Generally, the thickness of the graphene sheet is around 1 nm. Carbon Nano Tubes (CNT), Carbon nanotubes, a graphene nano foil with a honeycomb lattice of carbon atoms wound into hollow cylinders to form nanotubes of diameters as low as 0.7 nm for a single-layered and 100 nm for multi-layered CNT and length varying from a few micrometers to several millimeters. The ends can either be hollow or closed by a half fullerene molecule. The same graphene nano foils are used to produce carbon nanofiber as CNT but wound into a cone or cup shape instead of a regular cylindrical tube. Carbon black: An amorphous material made up of carbon, generally spherical with diameters from 20 to 70 nm. The interaction between the particles is so high that they bound in aggregates and around 500 nm agglomerates are formed (Ealias & Saravanakumar, 2017).

2.1.1.3. Inorganic nanoparticles

Inorganic nanoparticles are particles that are not made up of carbon. Inorganic nanoparticles have fascinated scientists for over a century and are now heavily utilized in biomedical sciences and engineering. Today these materials can be synthesized and modified with various chemical functional groups which allow them to be conjugated with antibodies, ligands, and drugs of interest and thus opening a wide range of potential applications in biotechnology, magnetic separation, pre-concentration of target analytes, targeted drug delivery, and vehicles for gene and drug delivery and more importantly diagnostic imaging as previously expressed by (Blondeau et al., 2005). Moreover, various imaging modalities have been developed over some time such as magnetic resonance imaging, computed tomography, positron emission tomography, ultrasound,

surface-enhanced Raman spectroscopy, and optical imaging as an aid to image various disease states. These imaging modalities differ in both techniques and instrumentation and more importantly require a contrast agent with unique physiochemical properties. This led to the invention of various nano particulates. Metal and metal oxide-based Nanoparticles are generally categorized as inorganic nanoparticles (Ealias & Saravanakumar, 2017).

2.1.1.3.1. Metal based

Nanoparticles that are synthesized from metals to Nanometric sizes either by destructive or constructive methods are metal-based. Almost all the metals can synthesize into their nanoparticles. Previously, D. Mubarak Ali, N.T., et al. synthesized silver and gold nanoparticles by using plant extract mediated synthesis and its antibacterial activity against clinically isolated pathogens. They reported that different metals were used for the synthesis of nanoparticles by the green synthesis method. The commonly used metals for nanoparticle synthesis are aluminum (Al), cadmium (Cd), cobalt (Co), copper (Cu), gold (Au), iron (Fe), lead (Pb), silver (Ag), and zinc (Zn). The nanoparticles have distinctive properties such as sizes as low as 10 to 100nm, surface characteristics like the high surface area to volume ratio, pore size, surface charge and surface charge density, crystalline and amorphous structures, shapes like spherical and cylindrical, and color, reactivity, and sensitivity to environmental factors such as air, moisture, heat, and sunlight, etc. (Ealias & Saravanakumar, 2017).

2.1.1.3.2. Metal Oxides based

The metal oxide-based nanoparticles are synthesized to modify the properties of their respective metal-based nanoparticles, for example, nanoparticles of iron (Fe) instantly oxidizes to iron oxide (Fe_2O_3) in the presence of oxygen at room temperature increasing its reactivity compared to iron nanoparticles. Metal oxide nanoparticles are synthesized mainly due to their increased reactivity and efficiency. The commonly synthesized are Aluminium oxide (Al_2O_3), Cerium oxide (CeO_2), Iron oxide (Fe_2O_3), Magnetite (Fe_3O_4), Silicon dioxide (SiO_2), Titanium oxide (TiO_2), Zinc oxide (ZnO). These nanoparticles have possessed an exceptional property when compared to their metal counterparts (Ealias & Saravanakumar, 2017).

2.2. Zinc Oxide Nanoparticles

Zinc oxide is a semiconducting inorganic material with three different crystal structures: Wurtzite, zinc blende, and rock salt. At ambient conditions, the structure of Wurtzite is thermodynamically stable, with every zinc atom being tetrahedrally coordinated with four oxygen atoms (Degefa et al., 2021). With a wide band gap of 3.1-3.3 eV, (Khalfa et al., 2019) zinc oxide has great potential for application in many fields, such as biosensors, cosmetics, drug carriers, and antibacterial agents (Basnet et al., 2018). ZnO can be synthesized by many different methods, such as sol-gel processing, homogeneous precipitation, mechanical milling, organometallic synthesis, the microwave method, spray pyrolysis, thermal evaporation, and mechanochemical synthesis (Haque et al., 2020). However, these kinds of methods usually use organic solvents and toxic reducing agents, the majority of which are highly reactive and harmful to the environment. Therefore, to minimize the impact on the environment, green synthesis processes have been used to synthesize ZnO NPs. Green synthesis is a method to produce nanoparticles using microorganisms and plants with biomedical applications. This method has many advantages, such as environmental friendliness, cost-effectiveness, biocompatibility, and safety. Additionally, many studies have proved that ZnO NPs made using green synthesis processes have strong antibacterial properties. Recently, ZnO NPs have been successfully synthesized using extracts from plants (Xu et al., 2021) synthesized ZnO NPs using Citrus sinensis peel extract and compared with commercial ZnO NPs and then applied as nanocoatings on fresh strawberries to evaluate the preservation effect. The high antibacterial and antifungal activities of ZnO NPs improve the potential in food packaging applications. (Doan Thi et al., 2020) has addressed the influence of different amounts of Orange fruit peel extract on the size and shape homogeneity of ZnO NPs. Besides, photocatalytic degradation of methylene blue (MB) under UV light of ZnO NPs presented a better rate than commercial ZnO NPs (Balcha et al., 2016). Found that ZnO NPs exhibited various size and shape distributions using *Lycopersicon esculentum* (tomato), *Citrus sinensis* (orange), *Citrus paradisi* (grapefruit), and *Citrus aurantifolia* (lemon) extracts. Most ZnO samples exhibited degradation rates of Methylene blue (MB) under UV light at 180 min of around 97% (Kalpana & Devi Rajeswari, 2018) evaluated different green fabrication methods for ZnO synthesis using *Coriandrumsativum* leaf extract. Although the different size and antioxidant activities, all the formed ZnO NPs had bactericidal effects against both Gram-negative and Gram-positive bacteria strains (Lakshmi et al., 2017). Also used both microwave irradiation and conventional heating to

synthesize ZnO NPs from Rosa canina fruit extract. The antibacterial activities of ZnO NPs with several bacteria such as Listeria monocytogenes, E. coli, and Salmonella typhimurium were investigated by Lakshmi et al (Lakshmi et al., 2017).

2.2.1. Properties of ZnO nanoparticle

Zinc oxide as a nonhygroscopic and nontoxic, inorganic, polar, crystalline material is a very cheap, safe, and readily available, which has aroused great interest in various organic transformations, sensors, transparent conductors, and surface acoustic wave devices (Darvishi et al., 2019). The ZnO NP is an exclusive material that has semiconducting, piezoelectric, and pyroelectric properties and has versatile applications in transparent electronics, UV light emitters, chemical sensors, spin electronics, personal care products, catalysts, coating, and paints (Darvishi et al., 2019). Due to its unique properties, ZnO NPs find applications in antireflection coatings, transparent electrodes in solar cells, UV light emitters, diode lasers, varistors, piezoelectric devices, surface acoustic wave propagators (Siddiqi et al., 2018) (Properties, 2013), as an antimicrobial agent (Gharpure & Ankamwar, 2020), as photonic material, and for gas sensing (Liewhiran & Phanichphant, 2007). The biomolecules in the plant extract act as efficient capping agents, thus playing a major role in NP synthesis. The capping agents seem to stabilize NPs through different mechanisms that include electrostatic stabilization, steric stabilization, stabilization by hydration forces, and stabilization using Vander Waals forces. The stabilization of NPs is significant for their functions and applications (Ajitha et al., 2016).

A. Structure of Zinc oxide nanoparticles

The structures of nanoscale zinc oxide can be classified among novel materials with latent applications in numerous fields of nanotechnology. Zinc oxide can arise in 1D, 2D, and three-dimensional (3D) structures. One-dimensional structures make upbeat the leading group, including, needles, nanorods helixes, rings and springs, ribbons, tubes, belts, combs, and wires. Zinc oxide can be obtained in 2D structures, such as nanosheets and nanoplate. Examples of 3D structures of zinc oxide contain flowers, coniferous, snowflakes, urchin-like, dandelions, etc. ZnO provides one of the greatest assortments of varied particle structures among all known materials (Parihar et al., 2018).

The crystal structures shared by ZnO are wurtzite, zinc blende, and rock salt (Figure 1). The wurtzite structure is most common and stable under ambient conditions. At ambient pressure and

temperature, ZnO crystallized in the wurtzite (B4 type) structure. This is a hexagonal lattice, belonging to the space group P63mc, and is characterized by two interconnecting sub lattices of

Zn^{2+} and O_2, such that each Zn ion is surrounded by tetrahedral O^{2-} ions, and vice-versa. This tetrahedral coordination gives rise to polar symmetry along the hexagonal axis. This polarity is responsible for a number of the properties of ZnO, including its piezoelectricity and spontaneous polarization, and is also a key factor in crystal growth, etching, and defect generation. The zinc blende ZnO structure can be stabilized only by growth on cubic substrates and the rock salt NaCl structure may be obtained at relatively high pressures. In both cases, the zinc and oxide centers are tetrahedral; the most characteristic geometry for Zn (II) (Parihar et al., 2018).

Hexagonal and zinc blende polymorphs have no inversion symmetry (reflection of a crystal relative to any given point does not transform it into itself). This and other lattice symmetry properties result in piezoelectricity of the hexagonal and zinc blende ZnO, and piezoelectricity of hexagonal ZnO.

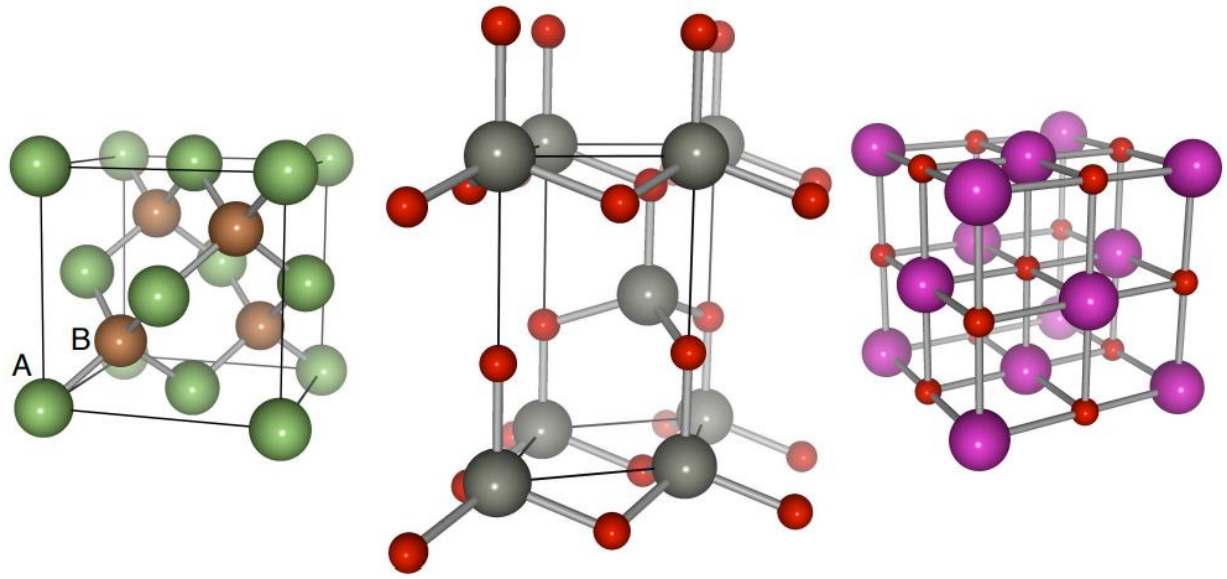

Figure 1 The crystal structures (left to right) zinc blende, wurtzite (ZnO), and rocksalt.

B. Mechanical properties

The mechanical properties of materials involve various concepts such as hardness, stiffness, piezoelectric constants, Young's and bulk modules, and yield strength. Piezoelectricity is the electric charge that accumulates in certain solid materials in response to applied mechanical stress. The word piezoelectricity means electricity resulting from pressure. The piezoelectric effect is understood as the linear electromechanical interaction between the mechanical and the electrical state in crystalline materials with no inversion symmetry. Among the tetrahedrally bonded semiconductors, it has been stated that ZnO has the highest piezoelectric tensor. This property makes it a technologically important material for many applications (Parihar et al., 2018)

C. Electronic properties

ZnO has a relatively large direct band gap of ~3.3 eV at room temperature; therefore, pure ZnO is colorless and transparent. Advantages associated with a large band gap include higher breakdown voltages, the ability to sustain large electric fields, lower electronic noise, and high temperature and high-power operation. The band-gap of ZnO can further be tuned from ~3.4 eV by its alloying with magnesium oxide or cadmium oxide (Kumar & Walia, 2015).

D. Optical properties

Intrinsic optical properties of ZnO nanostructures are being intensively studied for implementing photonic devices. Photoluminescence (PL) spectra of ZnO nanostructures have been extensively reported. From the photoconductivity measurements of ZnO nanowires, it is found that the presence of O_2 has an important effect on the photoresponse. It was found that the desorption-adsorption process of O_2 affects the photo response of ZnO nanowires. Upon illumination, photogenerated holes discharge surface chemisorbed O_2 through surface electron-hole recombination, while the photogenerated electrons significantly increase the conductivity. When illumination is switched off, O_2 molecules reabsorb onto the nanowire surface and reduce the conductivity (Sabir et al., 2014).

2.3. Synthesis Methods of Zinc Oxide Nanoparticles

The preparation of nanoscale structures and devices can be accomplished through "bottom-up" or "top-down" methods. In the bottom-up approach, small building blocks are assembled into larger

structures; chemical synthesis is a good example of the bottom-up approach in the synthesis of nanoparticles. In the top-down approach, large objects are modified to give smaller features, attrition or milling is a good example of a top-down approach. Both approaches play very important roles in modern industry and most likely in nanotechnology. Methods to produce nanoparticles from atoms are chemical processes based on transformations in solution e.g. sol-gel processing, chemical vapor deposition (CVD), plasma or flame spraying synthesis, and laser pyrolysis, atomic or molecular condensation. These chemical processes rely on the availability of appropriate "metal-organic" molecules as precursors (Cruz et al., 2020). In Figure 2 the synthesis approaches are also classified into physical, chemical, and biological synthesis depending on the processes or materials involved in the production process (Ealias & Saravanakumar, 2017).

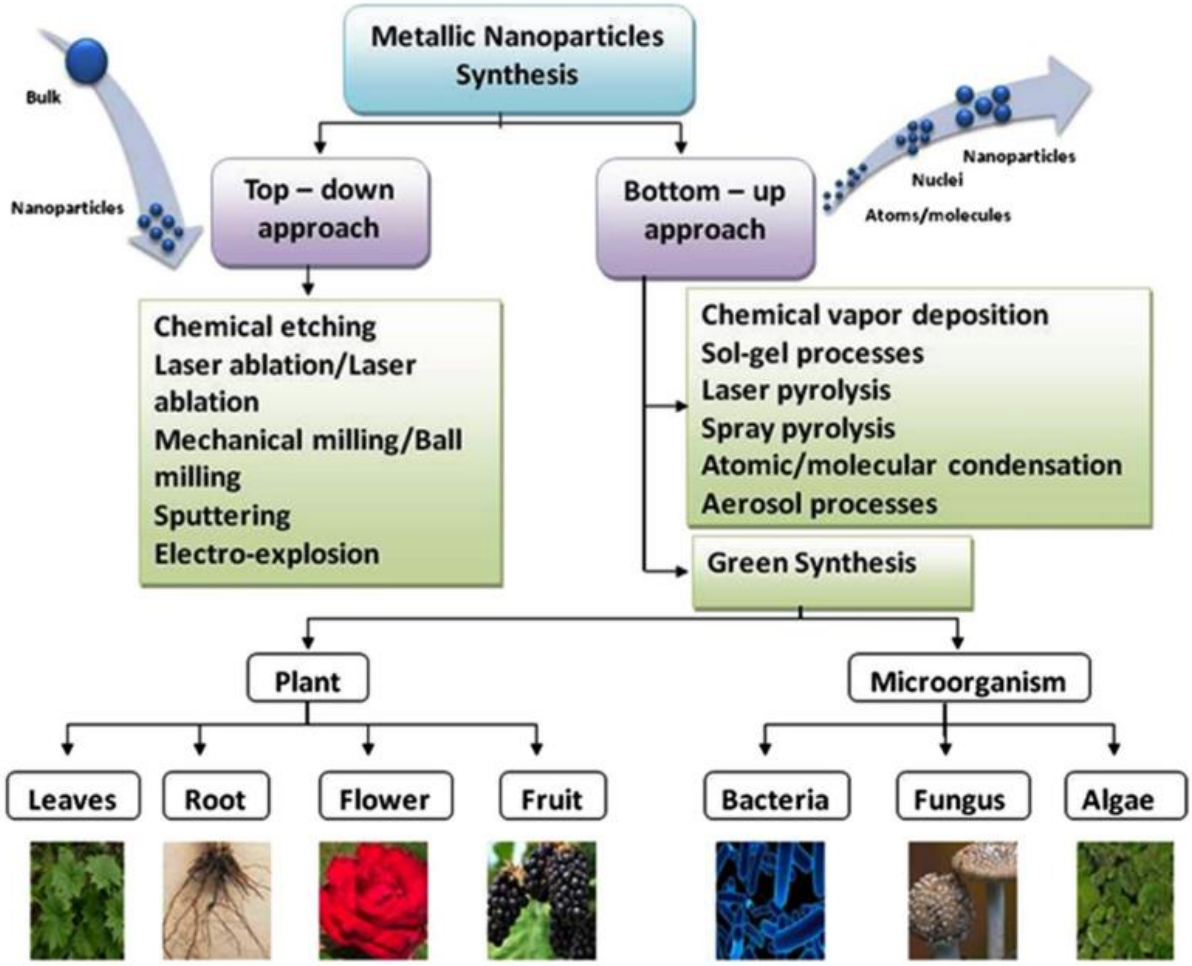

Figure 2 Different synthesis approaches used in metallic nanoparticles (Singh et al., 2018)

Recently, a strong focus is placed on green synthesis, where NPs are extracted from fungi, algae, bacteria, and plants (usually terrestrial) in which a variety of metabolites act as reducing agents in NPs synthesis. The advantage of using green synthesis is that they are easily available, safe, and versatile in the type of metabolites that could act as reducing and stabilizing agents. Additionally, different combinations such as plant extraction with the microwave irradiation method that heats the material through its dielectric loss are recently proposed (Cruz et al., 2020) (Doan Thi et al., 2020). The obvious increase in the alternatives for the synthesis of NPs and green approaches that use different biological materials is greatly encouraging.

2.3.1. Physical method

In the physical method, physical forces are involved in the attraction of Nanoscale particles and the formation of large, stable, well-defined nanostructures. The physical method is often called the top-down approach. It uses mechanical forces to break bulk particles or beams of atoms for the formation of nanoparticles. The physical method includes nanoparticle synthesis through, colloidal dispersion vapor condensation, amorphous crystallization, physical fragmentation and evaporation, pulse laser deposition, and sputtering. Physical synthesis methods are highly useful in producing ultra-thin and highly pure nanostructures and Nano alloys. The main shortcoming of the physical method is the use of costly equipment, high temperature, and pressure, and large space area for setting up machines (Gharpure & Ankamwar, 2020). Physical methods of ZnO nanoparticle synthesis include high-energy ball milling, melt mixing, physical vapor deposition, laser ablation, sputter deposition, electric arc deposition, and ion implantation. In most physical/mechanical processes, the production rates of ZnO nanoparticles are very high and are mostly used for industrial processes (Gharpure & Ankamwar, 2020).

2.3.2. Chemical method

The chemical method involves the use of toxic chemicals which can prove to be hazardous to the environment and the person handling it. These methods may result in toxic and harsh products which may pose biological risks to the environment; due to the high surface charge and high surface area of nanoparticles, harsh chemicals may remain adsorbed onto nanoparticles. Releasing these chemicals into the environment may cause adverse effects on organisms including microorganisms, plants, invertebrates, and vertebrates including humans at various trophic levels. These drawbacks have led to the emergence of green synthesis methods based on the use of environmentally friendly and biocompatible materials such as plants and microorganisms.

Therefore, it is essential to optimize green methods for nanoparticle synthesis (Gharpure & Ankamwar, 2020). Chemical methods need to use toxic chemical solvents such as reducing agents and these methods are expensive. Recently in nanotechnology, scientists wish for green synthesis with plant extracts, because this method has been useful and plays a very important role which is cheap, clean, safe, eco-friendly, non-toxic, and without any dangerous substance (Agarwal et al., 2017). Metal nanoparticles are usually synthesized using various chemical methods such as chemical reduction, solvothermal reduction, electrochemical techniques, and photochemical reactions in reverse micelles (Balantrapu & Goia, 2009). Among them, the chemical reduction is the most frequently applied method. Previous studies showed that the use of a chemical reducing agent resulted in the generation of larger particles and consume more energy. It was also reported that more side products were formed by chemical approaches which are not eco-friendly. Moreover, the chemically synthesized nanoparticles were reported to show less stability and more agglomeration (Cruz et al., 2020). Hence there is a need to develop an eco-friendly protocol that could produce stable and dispersible nanoparticles of controllable size by consuming less energy.

2.3.3. Green synthesis method

Green/biosynthesis of nanoparticles is an approach to synthesizing nanoparticles using microorganisms and plant applications. Green synthesis provides more advantages over physical and chemical methods biomedical because it is very cost-effective, non-toxic, uses safe reagents during the process, and eco-friendly technique due to the use of extracts from the plant (leaves, flower, seed, and peels), bacteria, fungi, and enzymes, as the reducing and stabilizing agents for the synthesis of nanoparticles instead of a large number of chemicals. This method does not require high temperature, high pressure, costly equipment, and hazardous chemicals (Gharpure & Ankamwar, 2020), (Espinosa et al., 2012). (Basnet et al., 2018) used *Allium sativum* leaf to synthesize ZnO NPs. The synthesized ZnO NPs were found to be spherical and the sizes were found to be 6nm (Ranganatha et al., 2019). (Agarwal et al., 2017) synthesized ZnO NPs using *Parthenium hysterophorus* leaves extract. In addition, the author evaluated the biosynthesized ZnO nanoparticles for Photodegradation of methylene blue, antimicrobial, and Catalytic activity. Hussein et al reported *Bacillus cereusas* as a biotemplate agent for the formation of ZnO NPs with raspberry and plate-like structures through a simple thermal decomposition of zinc acetate maintaining the original pH of the reaction mixtures. Baskar et al., 2013 produced ZnO NPs using

Aspergillus terreus filtrate synthesized extracellularly which were spherical with a range of 54.8 to 82.6nm (Hussein et al., 2009).

2.4. Characterization Technique

Nanoparticles and nanocomposites are generally characterized by thermal stability, size, optical properties, chemical composition, morphology, functional group, and surface charge, using advanced characterization techniques such as TGA-DTA, XRD, UV-Vis, SEM, FTIR, etc. The average particle diameter, size distribution, and charge affect the physical stability and the in vivo distribution of the nanoparticles. Particle size distribution and morphology are the most important parameters for the characterization of nanoparticles and nanocomposites (Akintelu & Folorunso, 2020).

Thermal stability and decomposition properties of materials are determined by using thermo-gravimetric analysis, crystal structure and average particles sizes using XRD, optical and electrical properties using UV-Vis, morphology, the size distribution, and shape using SEM and Transmission Electron Microscopy (TEM) (Akintelu & Folorunso, 2020). For SEM characterization, nanoparticles solution should be first converted into a dry powder, which is then mounted on a sample holder followed by coating with a conductive metal, such as gold, using a sputter coater. The sample preparation for TEM is complex and time-consuming because of its requirement to be ultra-thin for electron transmittance. The nanoparticle dispersion is deposited onto support grids or films. To make nanoparticles withstand the instrument vacuum and facilitate handling, they are fixed using either a negative staining material, such as phosphor tungstic acid or derivatives, uranyl acetate, etc. or by plastic embedding (Suresh et al., 2018).

2.5. Application of ZnO NPs

ZnO NPs, due to their above-mentioned unique or enhanced physicochemical properties, are used in a wide range of applications in different fields. In addition, several potential applications are in research and development. Here some examples of these applications were presents (Joudeh & Linke, 2022), (Kolodziejczak-Radzimska & Jesionowski, 2014).

2.5.1. Antimicrobial activity

2.5.1.1 Antibacterial activity

The antibacterial properties of ZnO NPs have become the focus of interest in pharmacy, biomedicine, and dentistry due to their low toxicity to humans and organisms. ZnO NPs can be selected as an antibacterial material because of their superior properties, such as high specific surface area and high activity to block a wide scope of pathogenic agents. But recently, the antibacterial activity of ZnO NPs is still scarcely known. Prior reports had suggested the main antibacterial toxicity mechanisms of ZnO NPs were based on their ability to induce excess reactive oxygen species (ROS) generation, such as superoxide anion, hydroxyl radicals, and hydrogen peroxide production. The antibacterial activity may involve the accumulation of ZnO NPs in the outer membrane or cytoplasm of bacterial cells and trigger Zn^{2+} release, which would cause bacterial cell membrane disintegration, membrane protein damage, and genomic instability, resulting in the death of bacterial cells (Jiang et al., 2016), (Doan Thi et al., 2020).

Biosynthesized ZnO NPs were tested against gram-positive bacteria such as *S. aureus*, *B. subtilis*, and gram-negative bacteria *E. coli*, *P. aeruginosa*, and *Salmonella paratyphoid*. Jiang et al. report the potential antibacterial mechanisms of ZnO NPs against *E. coli* (Jiang et al., 2016). It showed that ZnO NPs with an average size of about 30 nm caused cell death by directly contacting the phosphor lipids bilayer of the membrane, destroying the membrane integrity. The addition of radical scavengers such as mannitol, vitamin E, and glutathione could block the bactericidal action of ZnO NPs, potentially revealing that ROS production played a necessary function in the antibacterial properties of ZnO NPs (Doan Thi et al., 2020).

2.5.1.2 Antifungal activity

Emerging fungal infections and fungal contamination have been at the forefront of worldwide safety affairs in the last few years. Taking the food industry as a notable example, fungal contamination cannot only cause the deterioration of product quality, and economic loss but also severely threaten food safety and public health. Zinc oxide nanoparticles should exhibit good antifungal activity due to their unique nano-properties, including excellent bioavailability and self-sterilization (Sun et al., 2018). The synergistic antifungal activity of ZnO NPs was evaluated along with common antibiotics (e.g. ciprofloxacin, ampicillin, fluconazole, and amphotericin B). Their

inhibitory efficiency can be enhanced in combination with ZnO NPs, which could reduce the overuse of antibiotics (N. Sharma et al., 2016).

Barad et al. have shown that ZnO NPs coated with chitosan-linoleic acid have significant efficacy compared with fluconazole in inhibitory action on the growth and biofilm formation of *C. albicans* (Gharagozloo et al., 2015). It is worth noting that many filamentous fungi can produce secondary metabolites known as mycotoxins, which can induce immune suppression, as well as embryonic and even carcinogenic effects on human health. Thus, the most important application value of ZnO NPs lies in blocking and inhibiting the synthesis of mycotoxins (Savi et al., 2013).

For instance, the inhibitory performance of synthesized ZnO NPs on mycotoxin production was investigated by Hassan et al. They found that the existence of aflatoxigenic fungi and aflatoxin production was inhibited by the addition of 8 μg/mL of ZnO NPs, while the inhibitory results were also observed for ochratoxin A and fumonisin B1 when the concentration of ZnO NPs was increased to 10 μg/mL. These findings indicated that the involvement of ZnO NP in the food matrix may not only effectively inhibit the growth of harmful fungi, but importantly decrease the content of mycotoxins produced by toxigenic fungi (Hassan et al., 2013). Deepali et al. have found that the inhibitory action of ZnO NPs on the fungus (Fusarium sp.) was concentration-dependent, and this dependency was also affected by particle size (D. Sharma et al., 2010).

2.5.2. Antioxidant activity of ZnO NPs

The evaluation of the antioxidant activity of nanomaterials has become one of the significant basic studies in pharmaceutical science as well as in nanoscience and technology. Antioxidants play an important role in the functioning of all bio-systems. In biological systems, free radicals are generated due to the interaction of biomolecules with molecular oxygen. These free radicals are responsible for the degradation of biomolecules. Oxidation is also accountable for nutritional quality deterioration and discoloration of food. Consumption of oxidized foods generates lipid peroxides and low molecular weight compounds which cause serious diseases like hepatomegaly or necrosis of epithelial tissues. In the biological systems, antioxidant plays an important role in the scavenging of these toxic free radicals. Many kinds of natural and synthetic antioxidants have been investigated to inhibit these oxidation reactions to date (Das et al., 2013).

The 2, 2-Diphenyl-1-picrylhydrazyl (DPPH) scavenging assay is regarded to be the most widespread technique for studying the antioxidant property of materials. In this method,

antioxidant efficiency is measured at ambient temperature to eliminate the risk of thermal degradation of the molecules tested. Different researchers have examined the antioxidant activity of many kinds of natural as well as synthetic compounds (Das et al., 2013). Zhang and Xiong reported as DPPH, a stable free radical with a characteristic absorption at 517–520 nm was used to determine the radical scavenging activity of ZnO NPs prepared by using *G. xanthochymus* fruit extracts. The decrease in absorption at 520 nm was measured as the degree of radical scavenging. The radical-scavenging activity (RSA) values were expressed as the ratio of the percentage of sample absorbance decrease and the absorbance of DPPḢ solution in the absence of extract at 520 nm. The ZnO NPs were evidenced to be effective at the DPPH free radical scavenging activity with IC_{50} value of 800 mg/mL (Zhang & Xiong, 2015).

2.5.3. Photocatalytic activity of ZnO NPs

Over the past few years, the preparation of nanomaterials with divergent morphologies via green methods has given a boost to the application of these materials in catalysis and the manufacture of commercial products. Water sources have suffered unprecedented contamination due to the huge volume of organic dyes being discharged from textile industries. These dyes are mostly not biodegradable, toxic to the ecosystem, and carcinogenic to the cell. Various methods have been reported for the removal of dyes from solutions such as reverse osmosis, oxidation using a chemical action, membrane filtration, and coagulation and adsorption techniques. The materials used in these methods are either expensive or result in the formation of waste that is non-biodegradable and non-recyclable. In an attempt to overcome this snag, ZnO NPs synthesized via the green method are cheap and nontoxic nanoparticles that have a significant photocatalytic activity for dye removal (Balcha et al., 2016), (Akintelu & Folorunso, 2020).

Photocatalytic activity is based on the interaction between a photo-catalyst, usually a semiconductor, and light to produce reactive hydroxyl radicals or superoxide species that could interact with dye molecules, resulting in an enhanced degradation process of the organic dyes. ZnO NPs have been reported as good photocatalysts in the degradation of organic dyes due to their high stability, electron binding energy, and large surface area. They exhibit photo-catalytic degradation ability similar to TiO_2 due to their close bandgap energies; thus, an efficient alternative for the degradation of organic dyes and potential environmental pollutants. The nanoparticles have oxygen vacancy-induced bandgap narrowing which enhances their visible light photocatalytic activity (Balcha et al., 2016). ZnO is one of the most promising materials for executing the removal

of large quantities of cyanide, degrading pesticide, carbetamide, and herbicide and pulp mill bleaching wastewater, 2-phenyl phenol, phenol, methylene blue, and acid red as an alternative to the widely used, relatively expensive titanium oxide (TiO_2). This superiority of ZnO photo-catalytic activity is because its more active sites possess a high surface-to-volume ratio, vacancies and uncoordinated atoms at corners and edges, higher reaction rates, and are more effective in generating hydrogen peroxide. The mechanism of photocatalytic degradation of methylene blue could be illustrated thus: when incident UV light irradiated the ZnO nanoparticles, it created electron-hole pair via oxidation and reduction processes which ultimately generated -OH radicals in the presence of O_2. These photogenerated hydroxyl radicals and superoxide radicals were responsible for the photocatalytic degradation of methylene blue over ZnO NPs (Balcha et al., 2016)

2.5.4. Application of ZnO NPs in cosmetics

The rapid development of nanotechnology has resulted in an increasing number of nanomaterial-based consumer products and industries. Because of their unique physical properties, nanomaterials have dramatically transformed the function and application of commercial products, including wound dressings, cosmetics, detergents, food packaging, drug delivery, biosensors, and antimicrobial coatings. Recently, ZnO and TiO_2 nanoparticles have gained popularity as inorganic physical sunscreens because they can reflect and scatter UV radiations while preventing skin irritation and disruption of the endocrine system typically induced by chemical UV filters. Also, these NPs may be transparent and pleasant to touch (Lu et al., 2015). However, safety concerns regarding their utilization in consumer products have recently emerged. In literature, Li et al. report suggested that sunscreen NPs induce cytotoxicity and genotoxicity through oxidative stress. Physicochemical characterization of nanomaterials particle size, particle size distribution, aggregation, agglomeration state, shape, surface area, composition, surface charge, and solubility/ dispersibility were critical for the identification of test materials before toxicological assessment (Lu et al., 2015). The Advantages offered by sunscreens based on inorganic compounds comprise the absence of skin irritation and sensitization, inertness of the ingredients, limited skin penetration, and broad spectrum protection. The natural opaqueness of these micro-sized sunscreen components is eliminated without reducing their UV-blocking efficacy by utilizing nanosized ZnO and TiO_2 particles. Since the surface area to volume ratio of particles increases as the particle

diameter decreases, nanoparticles (NPs), i.e., nano-objects with all three external dimensions in the nanoscale, may be more reactive than normal bulk materials (Lu et al., 2015).

2.5.5. Biomedical application of ZnO NPs

ZnO NPs, as a new type of low-cost and low-toxicity nanomaterial, have attracted tremendous interest in various biomedical fields such as anticancer, antibacterial, antioxidant, Antidiabetic, sunscreen, and anti-inflammatory activities, as well as for drug delivery, bio-imaging and used as an ultraviolet (UV) radiation filter in sunscreen cosmetics (creams, balms, lotions) applications. ZnO NPs less than 100 nm are considered to be relatively biocompatible and biodegradability, which support their biomedical applications and represent a powerful property in promoting biomedical research (Kolodziejczak-Radzimska & Jesionowski, 2014) (Zhang & Xiong, 2015)

2.5.6. Agricultural applications of ZnO NPs

The continuous use of commercially available antibiotics in the treatment of farm animals has led to the development of multidrug-resistant strains of bacteria and fungi. The discovery and application of ZnO NPs in the treatment of fungi and other microbial infections in both farm animals and plants have been considered a better alternative when compared to conventional antibiotics. ZnO NPs have been reported to demonstrate excellent pesticide efficiency against *Artemia salina larvae* (Akintelu & Folorunso, 2020).

The potential of biosynthesized ZnO NPs as an antifungal and antibacterial agent in agriculture is traceable to the biomolecules found in the plant extracts used as reducing agents. Furthermore, findings have shown that the inorganic features of ZnO NPs have the efficiency to withstand the inhibition of microorganism growth at higher temperatures and other severe conditions when compared to numerous commercially available antibiotics. The small size to the large surface area, composition, and morphological nature of ZnO NPs enhance the interaction and penetration of ZnO NPs through the core cells of bacteria to damage and kill the cell. The fertility investigation of ZnO NPs in the growth of the *Arachis hypogea* plant showed an increase in seed germination, fast shoot growth, enhanced seedling vigor index, and rapid root growth; the flowering state was also fast, and a notable increase in the pod size and yield were recorded. Another study on the fertility efficiency of ZnO NPs on *Solanum lycopersicum* showed an increase in germination rate and increase in protein content. Several studies have reported the potential of ZnO NPs in increasing the yield of food crops (Akintelu & Folorunso, 2020).

2.6. *Coriandrum sativum* (Dimbilal)

A glabrous aromatic, herbaceous annual plant with a long history as a culinary herb, *Coriandrum sativum* (Figure 3) is the source of aroma compounds and essential oil with biologically active components that have different activities. As a result, *Coriandrum sativum* is useful in food preparation (as a flavoring agent and adjuvant), preservation, as well as in the prevention of food-borne illnesses and food spoilage (Mandal & Mandal, 2015). There are several regional names for it in Ethiopia, including dembilal (Amharic), Debo, shucar (Afanoromo), Tsagha, Zagda (Tigrignya), and Tibichota (Konsonya). A traditional spice known as "Data" that is consumed as a Wot, meat and fish is made from leaves and immature fruits of *Coriandrum sativum* (Kassahun, 2018).

Coriandrum sativum is an annual, herbaceous plant that grows 25 to 60 cm in height. It has thin, spindle-shaped roots, an erect stalk, alternate leaves with green or dark green (Figure 3), and small, pinkish-white flowers. The plant is grown widely all over the world for seed, as a spice, or for essential oil production. The whole or ground seed (fruit) is an ingredient of pickling spices also used to flavor various commercial foods, particularly, to prepare some instant chutneys, and sauces, in flavoring curries and soups. The green leaves of coriander are known as "cilantro" in the United States, (Asgarpanah, 2012). The fruit extract is used in lotions and shampoos as an antibacterial agent. Coriander leaves are widely used as a folk medicine as carminative, spasmolytic, and digestive. It has the advantage of being more stable and of retaining its agreeable odor longer than any other oil of its class (Asgarpanah, 2012).

Antioxidant, antibacterial, antifungal, antidiabetic, hepatoprotective, and antihyperlipidemic actions are just a few of the pharmacological properties of the *C. sativum* plant. According to Asgarpanah, who studied the anti-oxidative properties of *C. sativum* various components, the leaves exhibited greater antioxidant activity than the fruits. Total phenolic content in the extracts was shown to be positively correlated with antioxidant activity (Asgarpanah, 2012).

Figure 3 the photo of *Coriandrum sativum* (Dimbilal) plant leaf.

2.6.1. The composition of *Coriandrum sativum*

Coriandrum sativum leaf oil contains different compositions reported as Mandal like Decanal, trans-2-decenal, 2-decen-1-ol and cyclodecane, cis-2-dodecena, Dodecanal, dodecan-1-ol (Mandal & Mandal, 2015). Additionally, according to Asgarpanah, the leaf oil was primarily composed of aromatic acids, with 2-decanoic acid, E-11-tetradecenoic acid, capric acid, undecyl alcohol, tridecanoic acid, and undecanoic acid being the main components (Asgarpanah, 2012).

Fresh herbage and mature fruits have entirely different flavors and aromas. While oxygenated monoterpenes and monoterpene hydrocarbons are significant components in the oil recovered from *C. sativum* fruit, aliphatic aldehydes (mostly C_{10} to C_{16} aldehydes) with a fetid-like scent predominate in the fresh herb oil (Bhuiyan et al., 2009). Essential oil and fatty oil are the *C. sativum* fruits' main chemical components. The dried coriander fruit's essential oil concentration ranges from 0.03 to 2.6 %, while the fatty oil content ranges from 9.9 to 27.7 %. Crude fat, crude fiber, crude protein, and ash concentrations range from 11.5 to 21.3 %, 17.8 to 19.15 %, 28.4 to 29.1 %, and 4.9 to 6.0 %respectively (Bhuiyan et al., 2009).

CHAPTER THREE

3. MATERIALS AND METHODS

3.1. Study Site Description

The required *Coriandrum sativum* leaves were collected from the Awash Melkassa and Wolaita Zone, in Damote from personnel agriculture. Then, the leaf samples were kept under shadow drying until they become ready for grinding. Synthesis of ZnO NPs was done at the Chemistry Department research laboratory work station at ASTU. Characterization of the synthesized ZnO nanoparticles was done at Adama Science and Technology University (ASTU), Addis Ababa Science and Technology University, and Bahir Dar University. Finally, the antibacterial and antioxidant testing of ZnO NPs was done at the Department of Applied Biology and applied Chemistry research laboratory at ASTU, and also antifungal activity of ZnO NPs was done at the Department of Biology at Haramaya University.

3.2. Chemicals and Reagents

The reagents and chemicals that were used for this study were Zinc Nitrate ($ZnNO_3.6H_2O$ 99.9 %, analytical reagent, Trust Chemicals), Ethanol reagent (C_2H_5OH 96 %, Fmd, Ethiopia), distilled water, Wagner's reagent [Iodine (I 98.5% Loba Chemie PVT.LTD), potassium iodide (KI 99.8 %, Samir tech-chem PVT. LTD)], Ferric Chloride ($FeCl_3$ 97 %, Sigma aldria), Chloroform ($CHCl_3$ 99.8 %, Blulux), Sulfuric acid (H_2SO_4 98 %, Sigma Aldrich), Potato Dextrose Agar (PDA), Sabouraud Dextrose Agar (SDA), Molten Hilton Agar (MHA), Dimethyl Sulfoxide (DMSO 99.5 %, SRL), 2,2-diphenyl-1-picrylhydrazyl (DPPH 97%, Sigma Aldrich), Methanol (CH_3OH 99.8 %, Loba Chemie PVT.LTD), Ascorbic acid ($C_6H_8O_6$ 97%, Sigma Aldrich, Sodium Hydroxide (NaOH 99 %, SigmaAldrich). All the chemicals and reagents used for the preparation of ZnO NPs were purchased from the local market in Addis Ababa.

3.3. Materials and Instruments

The equipment and apparatus required for ZnO NPs synthesis were: Beaker, hot plate with a magnetic stirrer, magnetic bar, pH meter, micro oven, filter paper, vial. petri dish, aluminum foil, mechanical grinder, centrifuge (LC-O4C), measuring cylinder, centrifuge tube, furnace (SX-2.5-

10 BOX Type Resistance Furnace), refrigerator, crucible tongs, glass funnel, test tube rack, test tubes, dropper, volumetric flask (100, 250, and 500 mL), evaporating dish and electronic balance. Some of the instruments that were used in this study were XRD (XRD-7000, Shimadzu Co., Japan), UV–Vis spectroscopy (V-770 Dual-beam UV-VIS Spectrometer, Azzota Corp., USA), SEM (model JEOL JCM-6000plus, Japan), FTIR (FT/IR-6600typeA, JASCO), and TGA/DTA (model DTA-60H, Shimadzu Co., Japan).

3.4. Methods

3.4.1. Preparation of *Coriandrum sativum* leaf extract

Coriandrum sativum was collected from wolaita Zone, Damote, Southern Nations Nationality of People (SNNP) Regional state from personnel agriculture. Firstly, the leaf was washed and cleaned with distilled water and allowed to dry at room temperature under a shaded area until the moisture content was removed and ready for fine grinding. Then after, the extraction was done by taking 20 g of the leaf powder into a 1000 mL beaker followed by adding 500 mL distilled water (DH_2O) (Figure 4). Then it was covered with aluminum foil and heated at a constant temperature of 75 ℃ for 1 hour. After that, the extracted suspension was allowed to cool to room temperature followed by filtering and storing within an appropriate beaker. Finally, the extracted suspension was stored at 4 ℃ for further use in the synthesis of the zinc oxide nanomaterials.

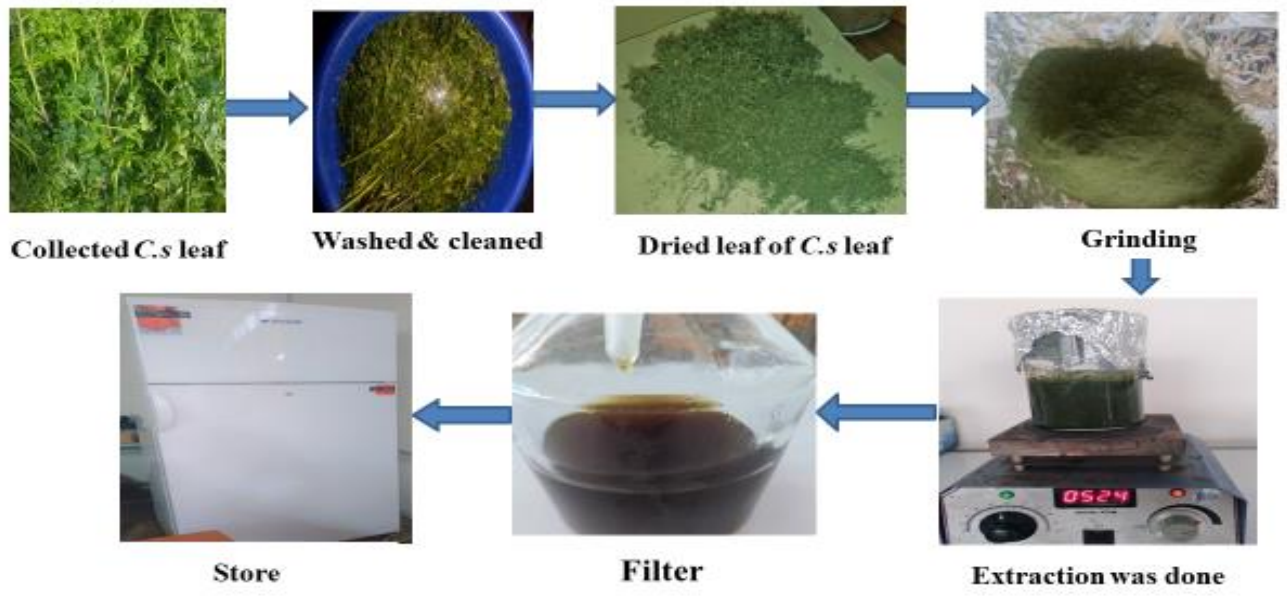

Figure 4 Preparation of *Coriandrum sativum* leaf extract.

3.4.2. Phytochemical screening of *Coriandrum sativum* plant leaf extract

3.4.2.1. Test for Flavonoids

5 mL of aqueous extracts of *Coriandrum sativum* leaf were treated with a 5 mL of 2 M sodium hydroxide (NaOH) solution (Shrivastava, 2017).

3.4.2.2. Test for Alkaloids (Wagner's test)

2 mL of leaf extract was mixed with 1 mL of Wagner's reagent prepared (1.27 g of iodine and 2 g of KI in 100 mL of distilled water) and shaken for 3 min (Shrivastava, 2017).

3.4.2.3. Test for Saponins

4 mL of plant extract was dissolved in 6 mL of distilled water and the mixture was shaken vigorously (Shrivastava, 2017).

3.4.2.4. Test for Tannins

3 mL of plant extract was dissolved in 3 mL of distilled water and a three drops of 2 % ferric chloride solution were added (Ashika et al., 2018).

3.4.2.5. Test for Phenol

5 mL of the extract was taken into a test tube and 7 drop of 2 % of $FeCl_3$ was added to an extract drop by drop wisely (Altemimi et al., 2017).

3.4.2.6. Test for Terpenoids

4 mL of aqueous extract of C. *sativum* leaf was dissolved in the 3 mL of chloroform. Then, 2 mL of concentrated sulfuric acid was added (Altemimi et al., 2017).

3.4.2.7. Test for Glycosides

2 mL of concentrated H_2SO_4 in the 5 mL of aqueous plant extract (Shrivastava, 2017).

3.4.2.8. Test for Steroids

2 mL of chloroform and concentrated H_2SO_4 were added with the 5 mL aqueous plant extract (Ashika et al., 2018).

3.4.2.9. Benedict test

2 mL aqueous plant extract was taken into a test tube and 3 drops of the benedict reagent was added drop by drop and heated for 2 min (Shrivastava, 2017).

3.4.3. Green synthesis of ZnO nanoparticles

ZnO NPs were synthesized as follows: First 0.4 M of zinc nitrate solution was prepared. The synthesis method was carried out within three volume ratio of extract and precursor salt: 50 mL of 0.4 M zinc nitrate solution was mixed with 50 mL of *Coriandrum sativum* leaf extract (CSLE) which have a 1:1 ratio, 60 mL of 0.4 M zinc nitrate solution was mixed with 40 mL of CSLE that is 2:3 ratio, and 40 mL of 0.4 M of zinc nitrate solution was mixed with 60 mL of CSLE (3:2) in 500 mL beaker for each ratio (Figure 5). Then the three samples were allowed to be stirred for about three hours by placed on a magnetic stirrer. Before stirring time completion at two hours and half an hour the pH of the solutions was checked using a pH meter and then after, a small amount of 1 M NaOH solution was added to reach a pH of 12 as pH control and as a precipitating agent. Then after the formed suspensions were placed within a refrigerator overnight. The suspensions were centrifuged at 2000 revolutions per minute (RPM) for 15 min to obtain nanoparticles. It was washed a minimum of three times followed by washing with DH_2O and ethanol within each step for each sample. After that, the samples were dried using a sample drying oven. The dried samples were calcined at 466 ℃ for two hours using the furnace. The samples were grind into powder and ready for the different characterization techniques.

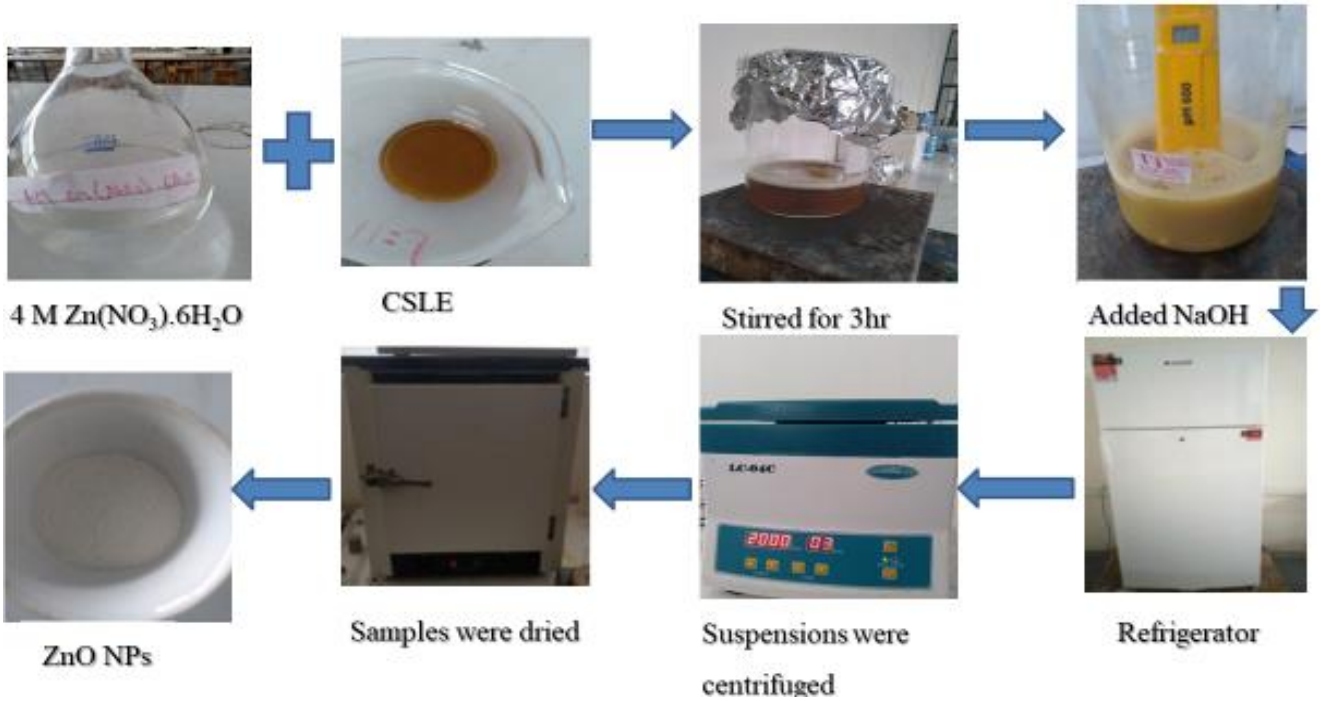

Figure 5 Synthesis of ZnO NPs using green synthesis method.

3.4.4. Characterization of ZnO nanoparticles

3.4.4.1. Thermal Analysis (TGA/DTA)

Thermal analysis was conducted to evaluate the thermal stability of ZnO NPs by using a TGA (model DTA-60H, Shimadzu Co., Japan). 10.171 mg of ZnO NPs samples were analyzed under 50 [mL/min] nitrogen flow rate with a heating rate of 10 ^{o}C at the temperature range of 22.74 to 1000 ^{o}C.

3.4.4.2. X-Ray Diffraction (XRD)

The formed nanomaterials were going to be characterized using XRD (XRD-7000, Shimadzu Co., Japan) equipped with a Cu target for generating a Cu Kα radiation with λ = 1.54056 Å XRD spectra were recorded from 10 ° to 80 ° for ZnO NPs with 2θ angles using Cu Kα radiation operated at 40 kV and 30 mA in continuous scan mode with scan rate 3 (deg/ min). This characterization method provided the average crystalline size of the synthesized nanoparticles. The average crystalline size (D) of the powders was calculated by using Scherrer's equation:

Debby's scherrer equation is indicated in the equation.

$$D = \frac{0.94\lambda}{\beta cos\theta}$$

Where K = 0.94 is Scherrer's constant, λ =1.5406 Å is the X-ray wavelength, θ is Bragg's diffraction angle, and β is the Full width at half maximum (FWHM) of the diffraction line at half of the maximum intensity.

3.4.4.3. UV-visible Spectroscopy (UV–Vis)

The optical properties of the ZnO NPs were determined by UV–Vis spectroscopy (V-770 Dual-beam UV-VIS Spectrometer, Azzota Corp., USA). The absorbance of samples was recorded in the wavelength range: of 200 to 800 nm and their maximum absorbance was recorded. Baseline correction of the spectrophotometer was carried out by using a blank reference. The UV-Vis absorption spectra of the samples were recorded.

3.4.4.4. Scanning Electron Microscopy (SEM)

The morphological features of the ZnO NPs were determined by using scanning electron Microscopy (model JEOL JCM-6000plus, Japan), using electron beam energy of 10 kV and magnification of 30.00 KX. Powdered samples were mounted on a sample holder followed by

coating with a smart coater (gold) and scanned. The surface characteristics of the samples were obtained from the secondary electrons emitted from the sample surface.

3.4.4.5. Fourier Transforms Infrared Spectroscopy (FTIR)

The functional groups present in dried powders of *Coriandrum sativum* leaf extract, uncalcinated ZnO NPs, and calcinated ZnO NPs were analyzed by an FTIR (FT/IR-6600typeA, JASCO). The spectra were acquired in the range 4000- 399.193 cm^{-1}.

3.4.5 Antibacterial activity

The antibacterial activity of biosynthesized ZnO NPs was carried out against four selected pathogens such as gram-positive (*Staphylococcus aureus* and *Streptococcus pyogen*) and gram-negative (*Escherichia coli* and *Pseudomonas aeruginosa*) bacteria in the Microbiology laboratory of ASTU by the disc diffusion method according to the procedure detailed by (Hudzicki, 2012).

3.4.5.1. Antibacterial assay of ZnO NPs

Antibacterial assay of ZnO NPs was performed by disk diffusion method in Mueller Hinton Agar (MHA) plates. The different concentrated solution was made by using the synthesized ZnO NPs of the three ratios (1:1, 3:2, and 2:3) in Dimethyl Sulfoxide (DMSO) (Hudzicki, 2012).

3.3.5.2. Preparation of ZnO NPs

For every three ratios of the synthesized ZnO NPs, 0.4 g were taken and dispersed in 1 mL DMSO. Thus 4 mg/mL of stock was obtained as a standard concentration of 50, 75, and 100 μg/mL concentration was taken and dispersed in 1 mL DMSO (Dadi et al., 2019).

3.3.5.3. Preparation of inoculum and McFarland standard

Bacterial cultures grown in the blood agar media at 37 °C for 24 h were adjusted to 0.5 McFarland which is approximately 1.5 $\times 10^8$ colony forming units (CFU/mL) (Hudzicki, 2012). The 0.5 McFarland standard was prepared by mixing 9.95 mL of 1 % H_2SO_4 in distilled water and 0.05 mL of 1 % $BaCl_2$ in distilled water to estimate bacterial concentration (Hudzicki, 2012). The preparation was kept in a flask and used for the contrast of bacterial suspension.

3.3.5.4. Disk diffusion assay

Two hundred microliter of a culture suspension of testing bacteria (approximately 1.5 $\times 10^8$ CFU/mL) was spread on Muller Hinton Agar (MHA) medium for bacteria. Sterilized filter paper disks (6 mm in diameter) soaked in ZnO NPs soaked filter paper disks were placed on the agar

plates which were inoculated with the tested bacteria. Amoxicillin (10 μg/mL) standard antibiotic disk was used as a positive control and 10 % Dimethyl Sulfoxide-soaked filter paper disks were used as the negative control. The plates were subsequently incubated at 37 °C for 24 h. After incubation, the growth inhibition zone was quantified by measuring the diameter of the zone of inhibition in mm (Dadi et al., 2019).

3.4.6. Antifungal activity

The antifungal activity of biosynthesized ZnO NPs was carried out against two selected pathogens such as *Aspergillus niger* and *Candida albicans* in the Biology department laboratory of Haramaya University.

3.4.6.1. Preparation of different concentrations of the ZnO NPs

The solutions (15, 20, and 25 mg/mL) of the ZnO NPs were prepared by reconstituting 0.015, 0.020, and 0.025 grams of each of the powders in 10 mL of DMSO. For preparing the 15 mg/mL, 20 mg/mL, and 25 mg/mL solutions of the nanoparticles were transferred to separate 10 mL capacity volumetric flasks (Peter et al., 2014).

3.4.6.2. Assay for antifungal activity of ZnO NPs

Antifungal activities of the synthesized ZnO NPs of the three ratios against *Aspergillus niger* and *Candida albicans* were determined using the disc diffusion method. First Potato Dextrose Agar (PDA) and Sabouraud Dextrose Agar (SDA) were prepared by dissolving the required amount of PDA and SDA powders with distilled water. Then the mixture was heated on a hot plate and autoclaved to get a boiled and uniform solution. The resulting autoclaved medium was transferred into separate Petri plates and allowed to solidify. Within 15 minutes of adjusting the turbidity of the suspension of inoculums, a sterile cotton swab was dipped into the adjusted suspension and rotated several times by pressing firmly on the inside wall of the tube above the fluid level. This removes excess fluid from the swab. Then, the dried surface of PDA and SDA plates was inoculated by streaking using the swab three times over the entire surface by rotating the PDA and SDA plates at approximately 60° each time to ensure an even distribution of the inoculums. Then, the PDA and SDA plates were left open in the hood for three to five minutes to allow for any excess surface moisture to be absorbed (Tsukatani et al., 2012). For the application, discs of 6 mm diameter were prepared from sterile filter paper cut into small, circular pieces of equal size by a perforator and then they were impregnated each with 0.01 mL of the prepared test powders.

The nanoparticles-impregnated discs were placed onto the surface of the inoculated agar plates using sterile forceps. Each disc was pressed down to ensure complete contact with the agar surface. The discs were distributed evenly so that they were no closer than 24 mm from center to center (Tsukatani et al., 2012). Discs of commercial Ketoconazoale /Tilt (10 units/disc) were used as positive controls while DMSO-impregnated discs were used as negative controls. Then the PDA and SDA plates were sealed with Parafilm and incubated at 27 °C for 5 to 7 days for fungal pathogens. After incubation, the diameters of the zone of inhibition around each disc were measured to the nearest millimeter along two axes (i.e. 90° to each other) using a transparent ruler and the means of the two readings were recorded. For each selected pathogen the experiment was carried out with three replications (Biswas et al., 2013).

3.4.7. Antioxidant activity

Antioxidant activity of Synthesized ZnO NPs was measured using the 2, 2-diphenyl-1-picryl-hydrazyl (DPPH) method. First, prepare the three ratios (1:1, 2:3, and 3:2) ZnO NPs stock solution by taking 8 mg of ZnO NPs added to 5 mL of methanol from this the serial solution was done at concentrations of (50, 100, 200, 400, and 800 µg/mL) second DPPH was prepared in methanol by dissolving 4mg DPPH in 100 mL methanol). Then, to each 1 mL of the above concentration solution were added each 4 mL of 0.04 % DPPH which was given 10, 20, 40, 80, and 160 µg/mL. The resulting solution was placed in the dark area for 30 minutes. Finally, ZnO NPs scavenging activity was also studied using various concentrations (50, 100, 200, 400, and 800 µg/mL) to study the absorbance trend. UV-vis absorbance at 517 nm was recorded and DPPH scavenging activity is calculated using the following equation (Safawo et al., 2018).

$$\text{Scavenging Activity (\%)} = \frac{\text{the absorbance of the control} - \text{Absorbance of sample at 517 nm}}{\text{absorbance of control}} * 100$$

CHAPTER FOUR

4. RESULTS AND DISCUSSION

4.1. Phytochemical Screening of *Coriandrum sativum* leaf Extract.

Coriandrum sativum leaf extracts were rich in different phytochemicals (Table 1 and Figure 6) with different functional groups that act as a capping agent.

In the present study, the qualitative analysis of *Coriandrum sativum* aqueous leaf extracts was carried out. Flavonoids, saponins, tannins, phenol, Steroids, and Benedict compounds were revealed to be present in extracts of *Coriandrum sativum* which are known to have antimicrobial activity (Laribi et al., 2015). Most of the phytochemicals from plant sources such as phenolic and flavonoids have been reported to have high content associated with their antioxidant activities and antibacterial that play a role in the prevention of the development of bacterial disease, particularly caused by oxidative stress (Ashika et al., 2018). Ashika et al., report on preliminary screening for phytochemicals in the *Coriandrum sativum* leaf extracts revealed the presence of phenolic, saponins, tannins, and flavonoids which could confer antibiotic properties on the plant. Therefore, the phytochemical screening result reveals that the presence of these phytochemical constituents supports the use of the *Coriandrum sativum* plant in folklore medications and it is probable that these phytochemicals are responsible for the healing properties of these plants which have been claimed by the peoples in the area of this study (Ashika et al., 2018).

These phytochemical species also play a critical role in nanoparticle synthesis to prevent agglomeration. XRD results showed that increasing the volume of plant extract causes the formation of small particle-size nanoparticles.

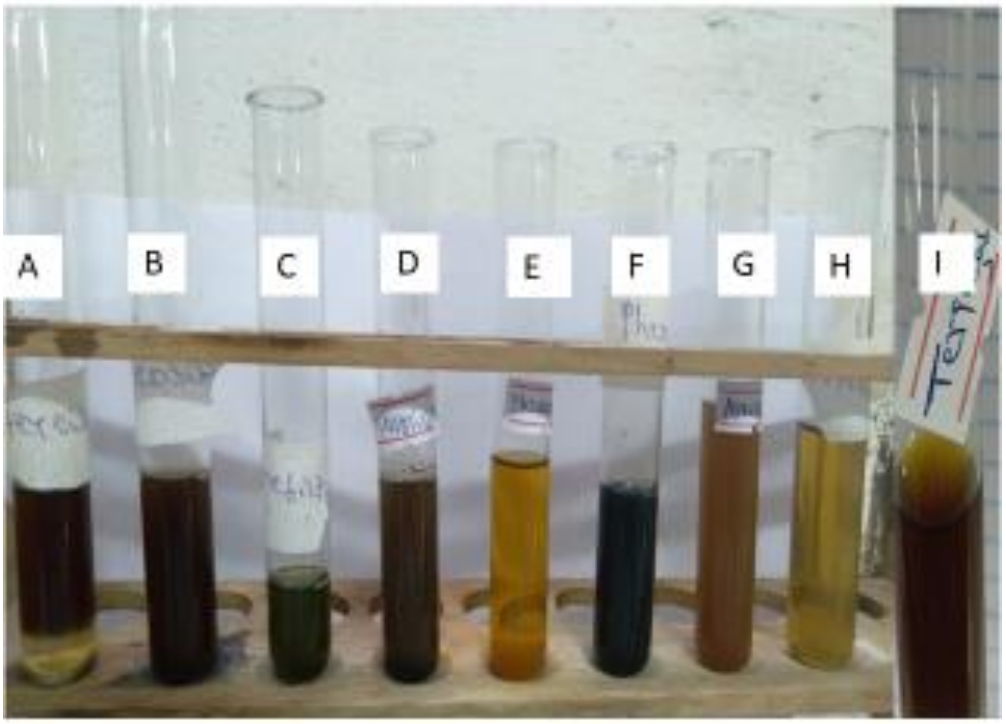

Figure 6 phytochemical test for aqueous extract *C. sativum* leaf to steroids (A), glycosides (B), benedict (C), taninns (D), flavonoids (E), phenol (F), alkaloids (G), saponins (H), and terpenoids (I).

Table 1 Results of phytochemical screening of aqueous extracts of *Coriandrum sativum* leaf.

S.no	Secondary Metabolite	Results	Colors observed
A	Steroids	+	Red color with chloroform layer
B	Glycosids	+	Reddish – brown
C	Benedict	+	Blue-green
D	Taninns	+	Brownish – green
E	Flavonoids	+	Yellow
F	Phenol	+	Dark green
G	Alkaloids	-	Not show reddish brown precipitate
H	Saponins	+	Stable persistent froth
I	Terpenoids	+	Reddish – brown

4.2. Characterization Analysis

4.2.1. Thermal Analysis (TGA/DTA) of ZnO NPs

The thermal analysis of the synthesized sample was investigated with TGA/ DTA analytical instrument. Thermal decomposition associated with the annealing process and the stability of the biosynthesized ZnO NPs analysis were measured from 23 to 1000 °C which were studied using simultaneous thermogravimetric analysis (TGA) and differential thermal analysis (DTA) at the heating rate of 15 °C/ min. The TGA curve shows the mass loss of the sample, whereas the DTA curve indicates the energy gain or loss during the process.

Figure 7 shows the TGA/DTA result of bio-synthesized ZnO NPs. The TGA curve shows an initial weight loss of ~ 30 % between 41.11 and 210.77 °C. The TGA derivative, not shown in the figure, revealed that this stage of weight loss contains two decomposition steps at 41.11 and 210.77 °C due to dehydration of adsorbed water and decomposition of organic binder from $Zn(OH)_2$. The second weight loss of 67 % from 210.77 to 466.24 °C can be attributed to the complete formation of pure ZnO NPs and the degradation of the organic compounds. The corresponding DTA curve showed three endothermic peaks at 56.97, 149.73, and 507.08 °C temperatures. DTA curve also showed two exothermic peaks at 294.41 and 895.94 ºC due to sample decomposition of $Zn(OH)_2$ to form ZnO and organic binders. The exothermic peak observed at 895.94 °C on the DTA curve might be due to the phase transition into a stable form of ZnO NPs, and no considerable loss in mass is observed after 466.24 °C temperature up to 1000 °C. This indicates that the biosynthesized ZnO NPs are thermally stable after 466.24 °C, so could be calcined at this temperature.

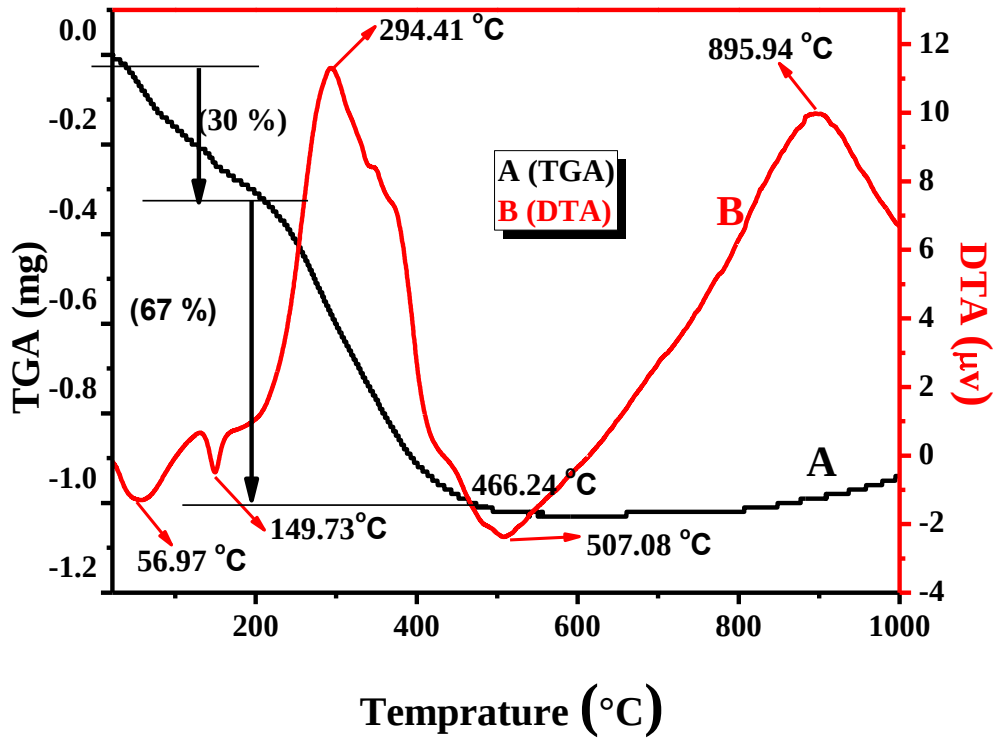

Figure 7 Thermal analysis of synthesized ZnO NPs (1:1) ratio.

4.2.2. X-Ray Diffraction (XRD) of ZnO NPs analysis

The analysis of a crystal phase and average crystalline size of the synthesized ZnO nanoparticles prepared through the green method using *Coriandrum sativum* leaf extract was done with an X-ray diffractometer. XRD data was taken for the prepared samples of ZnO NPs with an X-ray diffractometer at room temperature. ZnO NPs were formed from the reduction of zinc nitrate in the presence of *Coriandrum sativum* leaf extract, which acts as a reducing, stabilizing, and capping agent.

The four distinct results correspond to the different three volume ratios of precursor solution and one ratio calcination. The four distinct XRD patterns correspond to the different volume ratios of precursor solution and *Coriandrum sativum* leaf extract within a ratio of 1:1UC (uncalcinated), 2:3UC, 3:2UC, and 1:1C (calcinated) respectively for ZnO nanoparticles were depicted in Figure 8. By referring to Figure 8, the peaks at 2θ obtained from ZnO NPs peaks at 31.77°, 34.49°, 36.38°, 47.72°, 56.79°, 62.92°, 68.16°, and 69.26°. The results also confirmed the h k l values were (100), (002), (101), (102), (110), (103), (112), and 201 respectively for the ZnO crystals. This indicates that the peaks belong to the hexagonal Wurtzite structure ($P6_3mc$) and the synthesized ZnO NPs

possess a good crystallite structure as reported by (Zare et al., 2018). Intense Bragg peaks obtained suggest that strong scattering of X-ray is focused in the crystalline phase and may result from the presence of *Coriandrum sativum* as a capping and stabilizing agent (Vishwakarma et al., 2013). The average size for the different volume ratios (1:1UC, 1:1C, 2:3UC, and 3:2UC) was found to be 15.77, 19.59, 17.34, and 13.40 nm, respectively. The average crystalline size of 3:2 is less than that of 2:3. This is because 3:2 has less precursor salt and higher *Coriandrum sativum* leaf extract than that of 2:3. ZnO NPs biosynthesized within a volume ratio of 1:1 shows narrow diffraction peaks, indicating that it has a good crystalline structure as compared to the remaining ratio of synthesized ZnO NPs; because it has equal amounts of precursor salt and plant extract. However, in the diffraction patterns of the ZnO synthesized within a volume ratio of 3:2 decrease in the intensity and a widening of the diffraction peaks are observed as compared to the 1:1 sample, which is attributed to the decrease in the size of the crystals because of low concentration of precursor salts were present in the samples. The diffraction pattern of ZnO formed within a 2:3 ratio is rigid and narrow diffraction peaks are observed as compared to ZnO synthesized within a 1:1 volume ratio.

Table 2 also shows that the average crystal size of uncalcined ZnO NPs synthesized by using 1:1 ratios by volume of precursor salt and plant extract was less than their corresponding calcined ZnO NPs. This may also be due to the high concentrations of bio-molecules from plants that remain in the uncalcined NPs that could highly stabilize the nanoparticles by capping and hindering further crystal growth. This study agrees with a previous report (Demissie et al., 2020). The XRD results suggest that there was a systematic increase in peak intensity and peak width (FWHM) for calcined ZnO NPs than uncalcined ones. In addition, the peak intensity and peak width for ZnO (1:1) NPs decreased and increase in ZnO (2:3).

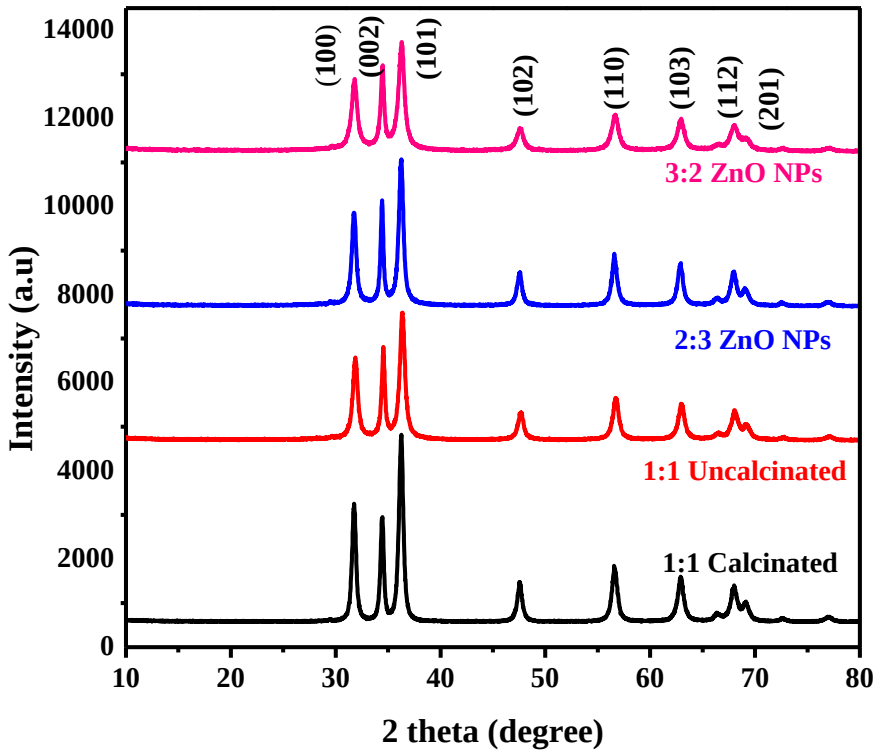

Figure 8 XRD patterns of ZnO nanoparticles synthesized under different ratios of zinc nitrate salt and *Coriandrum sativum* leaf extract.

Table 2 Structural parameters of prepared ZnO nanoparticles.

			1:1 CZnO NPs			1:1 UCZnO NPs			2:3 UCZnO NPs			3:2 UCZnO NPs		
No	h k l	d-spacing (d h k l)	2θ(°)	FWHM (°)	D(nm)	2θ(°)	FWHM (°)	D(nm)	2θ(°)	FWHM (°)	D(nm)	2θ(°)	FWHM (°)	D(nm)
1	1 0 0	2.81362	31.7676	0.4638	18.60	31.885	0.5812	14.85	31.7674	0.5124	16.83	31.8025	0.6626	13.02
2	0 0 2	2.59826	34.4422	0.4638	18.73	34.5535	0.5812	14.95	34.4299	0.5124	16.95	34.469	0.6626	13.11
3	1 0 1	2.46730	36.2485	0.4638	18.82	36.3683	0.5812	15.03	36.2476	0.5124	17.04	36.283	0.6626	13.18
4	1 0 2	1.90402	47.545	0.4638	19.55	47.6489	0.5812	15.60	47.5261	0.5124	17.69	47.5771	0.6626	13.68
5	1 1 0	1.61974	56.589	0.4638	20.32	56.6974	0.5812	16.22	56.5705	0.5124	18.39	56.6227	0.6626	14.22
6	1 0 3	1.47592	62.8729	0.4638	20.97	62.9497	0.5812	16.74	62.8408	0.5124	18.97	62.8901	0.6626	14.68
7	1 1 2	1.37451	67.9736	0.4638	21.58	68.0573	0.5812	17.22	67.9224	0.5124	19.52	68.0161	0.6626	15.10
8	2 0 1	1.35536	69.1015	0.5528	18.22	69.2015	0.6458	15.61	69.0015	0.7538	13.37	69.0215	0.98	10.27
9	Average crystallite size				19.59			15.77			17.34			13.40

4.2.3. UV-Vis spectrophotometric analysis of ZnO NPs

The biosynthesis of ZnO NPs from different ratios of ZnO $(NO_3).6H_2O$ and *Coriandrum sativum* plant leaves extract results are shown in Table 3. ZnO NPs synthesized from different ratios showed different results. The products with the different results obtained might be due to the formation of ZnO NPs with different sizes and optical properties.

Table 3. The effects of the plant extract on the optical properties and sizes of ZnO NPs.

No	The volume of *Coriandrum sativum* leaves extract (mL)	Volume of 0.4 M ZnO $(N0_3).6H_2O$ (mL)	Extract to Precursor ratio	UV–visible spectra of wavelength (nm)	The bandgap energies (eV)	Nano size (nm)
1	40	60	2:3	319.84	3.03	17.34
2	50	50	1:1	318.44	3.05	15.77
3	60	40	3:2	315.88	3.17	13.40

As can be observed from Table 3, changes in plant extract concentration cause changes in optical properties and particle size of ZnO NPs. As plant extract concentration increase, the nanoparticles size decrease; this causes a shift of absorption edge to the shorter wavelength or higher energy.

Figure 9A shows the UV–visible spectra of the ZnO NPs prepared using different concentrations of the plant extract and ZnO $(NO_3).6H_2O$ precursor. ZnO powder suspension in de-ionized water showed strong absorbance peaks in the range of 315.88-319.84 nm. The absence of other absorbance peaks in the spectra confirms that the synthesized materials were pure ZnO NPs. The occurrence of these absorption peaks was due to the surface plasmon resonance property of the nanoparticles, which occurs due to the oscillations of free electrons on the surface of the nanoparticles when they align in resonance with the wavelength of irradiated light. In the present study, increasing the volume of the plant extract was used to optimize the size of the ZnO NPs synthesized. A decrease in particle size was observed when increasing the volume of plant extract from 40 mL to 60 mL. Furthermore, the peak positions of UV-visible spectra are related to the size of nanoparticles and blue shifted or shifted to lower wavelength or higher energy as the crystal size of the nanoparticles decreased. The wavelength of maximum absorption and particle size have

a strong correlation. However, a further increase in extract volume resulted in a substantial broadening of the absorbance peak. This might be due to the increase in absorbance which could be attributed to the smaller particle size of ZnO NPs, which in turn increases its Rayleigh scattering ray. Different volumes of extracts contain different concentrations of organic binder. This indicates that at higher extract concentrations, the biomolecules act as reducing agents and cap the nanoparticles' surfaces protecting them from aggregation.

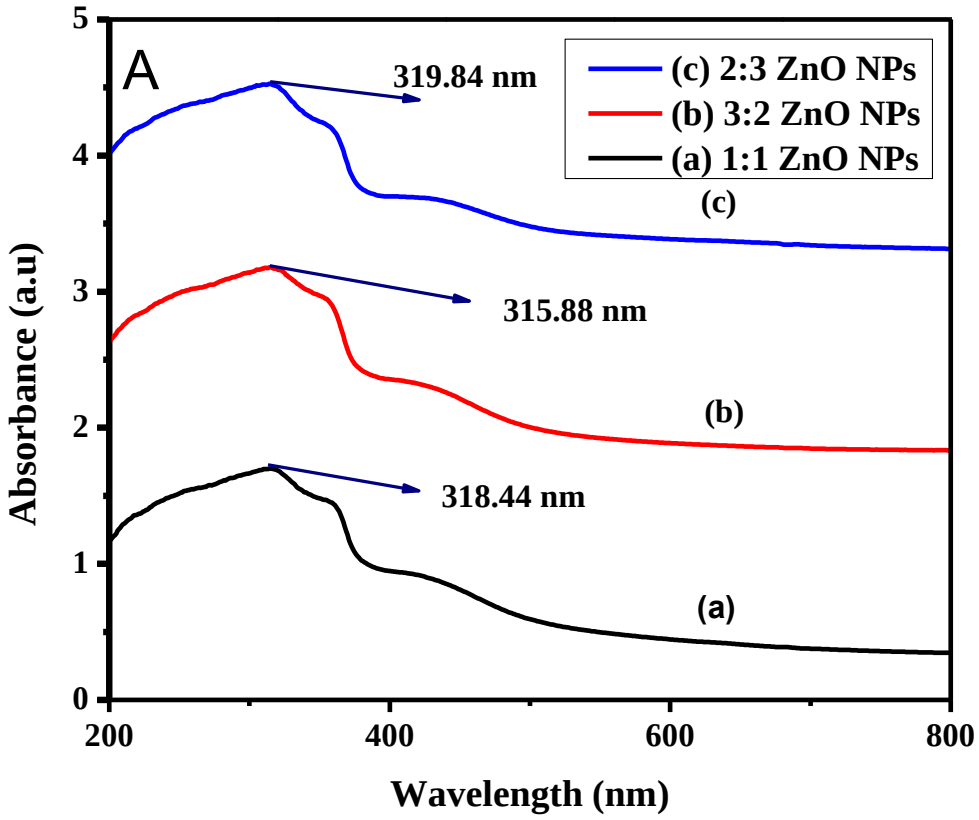

Figure 9 UV-Vis absorption spectra (A) for ZnO NPs synthesized by different ratios of plant extract to precursor solution.

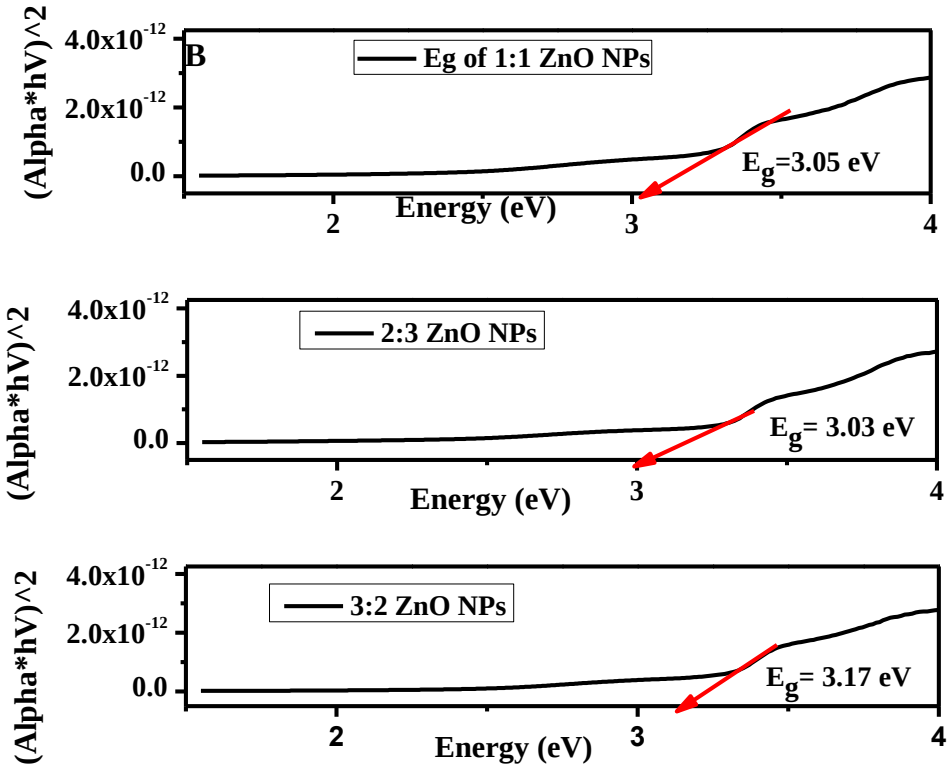

Figure 10 The energy band gap determination (B) for ZnO NPs synthesized by different ratios of plant extracts to precursor solution.

Utilizing Tauc's relationship between the optical absorption coefficient, the photon energy (hv), the constant alpha (α), and the direct band-gap energy (Eg), the bandgap energies were determined based on the numerical derivative of the optical absorption coefficient (Figure 10). In close agreement with previously reported values, band-gap energy values for ZnO NPs synthesized from 1:1, 2:3, and 3:2 ratios, respectively, were determined to be 3.05, 3.03, and 3.17 eV (Demissie et al., 2020).

4.2.4. Fourier Transforms Infrared Spectroscopy (FTIR) analysis

FTIR measurements were carried out to identify the possible bio-molecules responsible for the reduction of zinc nitrates. Figure 11 shows the FTIR spectra of green synthesized ratios of 1:1 calcinated, uncalcinated ZnO nanoparticles, and *Coriandrum sativum* leaves powder. The FTIR measurements were collected to find biomolecules for capping and the proficient stabilization of the zinc oxide nanoparticles synthesized by *Coriandrum sativum* leaves extracts. The spectra were recorded in the series of absorption bands 4000 – 400 cm^{-1}.

Figure 11 CZnO shows the FT-IR spectra of calcinated ZnO nanoparticles the O-H stretch appears in the spectrum as a very broadband extending from 3417 cm^{-1}. This very broad O-H stretch band is observed with a C=O peak, which almost certainly indicates that the compound is an aliphatic carboxylic acid. The band observed at 1632 cm^{-1} corresponds to the carbonyl group of flavonoids as reported by (Kumar, 2017) that revealing the peak to be 1415 cm^{-1}. An absorption peak found at 1058 cm^{-1} corresponds to saturated primary alcohol C-O stretching which is within the range reported that is from 1000 cm^{-1} - 1300 cm^{-1} (Kumar, 2017). The FTIR spectrum of zinc oxide (ZnO) nanoparticles absorbs at 660 cm^{-1} as reported by (Vishwakarma et al., 2013) ranging from 400-800 cm^{-1} while (Kumar, 2017) reported a range from 518 - 664 cm^{-1} as the presence of ZnO NPs. Thus, it can be observed from the FTIR spectrum that calcined ZnO NP is significantly rich in different chemical groups such as primary alcohols, alkanes, carboxylic acids, and flavonoids.

Figure 11 UCZnO shows the FT-IR spectra of uncalcinated ZnO nanoparticles. As it can be seen the peak at 818 cm^{-1} indicates stretching vibrations of Zn-O bond matching as the results reported by (Vishwakarma et al., 2013) ranging from 400-880 cm^{-1}. The O-H stretch appears in the spectrum as very broadband extending from 3425 cm^{-1}. This very broad O-H stretch band is observed with a C=O peak, which almost certainly indicates that the compound is an aliphatic carboxylic acid and also indicates water and phenol. Prominent levels of absorption observed at 2083 cm^{-1} reveal the presence of C–H stretching vibrations of an aromatic aldehyde. The peak observed at 1625 cm^{-1} corresponds to the C=O peak, which indicates the ketone functional group and also indicates the ammine functional group. The band observed at 1369 cm^{-1} corresponds to the carbonyl group of flavonoids (Suresh et al., 2018). An absorption peak found at 1058 cm^{-1} corresponds to saturated primary alcohol C-O stretching. Figure 11 Cs Leaves extract indicates absorption bands of *Coriandrum sativum* leaves extract the weak absorption peaks at 3386 cm^{-1} for OH band stretching mode, which is phenol. The absorption at 2913 cm^{-1} is aromatic C-H band stretching mode. The peak at 2858 cm^{-1} corresponds to a primary amine. The absorption at 2346 cm^{-1} indicates amide (C≡N). The peak at 1733 cm^{-1} shows C=O functional groups. The absorption at 1617 cm^{-1} can be assigned to the aromatic C=C stretching mode. The peak at 1407 cm^{-1} indicates flavonoid. Finally, the absorption at 570 cm^{-1} shows the stretching mode of C-O. The *Coriandrum sativum* leaf powder contains a polyphenolic compound with antioxidant potential. As compared to calcined ZnO NPs the FT-IR spectra of uncalcined ZnO NPs displayed a number of absorption peaks like primary alcohols, phenols, alkanes, water, carboxylic acids, flavonoids, ammine, CO_2,

aldehydes, amides and ketones. This might be due to chemically bonded functional groups of *Coriandrum sativum* leaves powder extract used as a capping agent during the synthesis of the materials which was not removed by washing with deionized water and ethanol. During the calcination process water, CO_2, phenols, ethanol, some ammines, and amides are removed (Hossain et al., 2019).

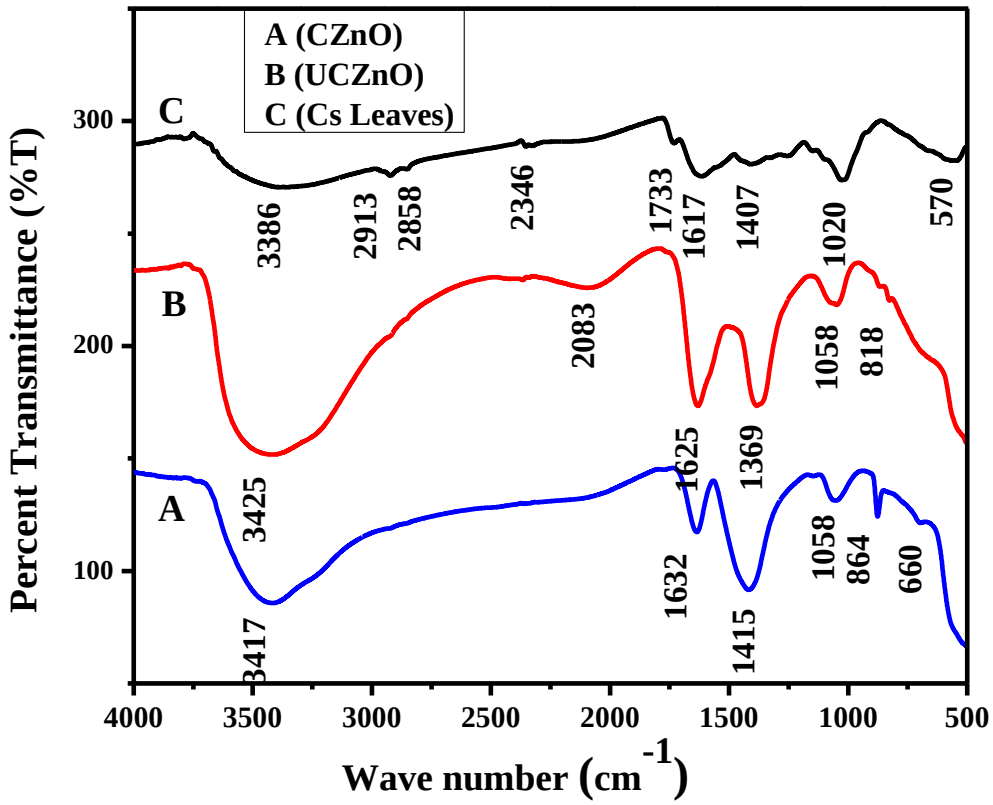

Figure 11 FT-IR spectrum for ZnO NPs calcined A (CZnO), uncalcined ZnO NPs B (UCZnO), and Coriandrum sativum leaf extract C (Cs Leaves).

4.2.5. Scanning Electron Microscopy (SEM) analysis

The scanning electron microscope results confirmed the surface morphologies of biosynthesized ZnO NPs and the results are presented in Figure 12 (a-c) for the volume ratios 1:1, 3:2, and 2:3.

Figure 12 (A) the morphology of ZnO NPs synthesized from 1:1 ratios by an equal volume of reactants its SEM images indicate the particles are almost spherical. The particles were agglomerated to form a sponge-like bunch of particles. This agglomeration could be induced by densification resulting in narrow space between particles. Figure 12 (B) shows the SEM image of

synthesized ZnO NPs 3:2 ratio. The image shows spherical shapes and is more deeply homogenized than the other counterpart of synthesized NPs due to the presence of a more capping agent that stabilizes the NPs and due to the presence of more leaf extract that stabilizes the formation of NPs and prevents their aggregation. The agglomeration of the particles is dependent upon the nature of compounds present in the extracts and attraction between the biomolecules and metal salts resulted in the aggregation of the NPs. In addition to this, the morphology of ZnO NPs synthesized from a 2:3 ratio the amount of the salt precursor is much greater than the amount of plant extract Figure 12 (C), which, contains both nanorod and flake-type shapes in aggregated form. In the previous report, this aggregation /agglomeration may be caused due to polarity and electrostatic attraction of ZnO nanoparticles (Demissie et al., 2020).

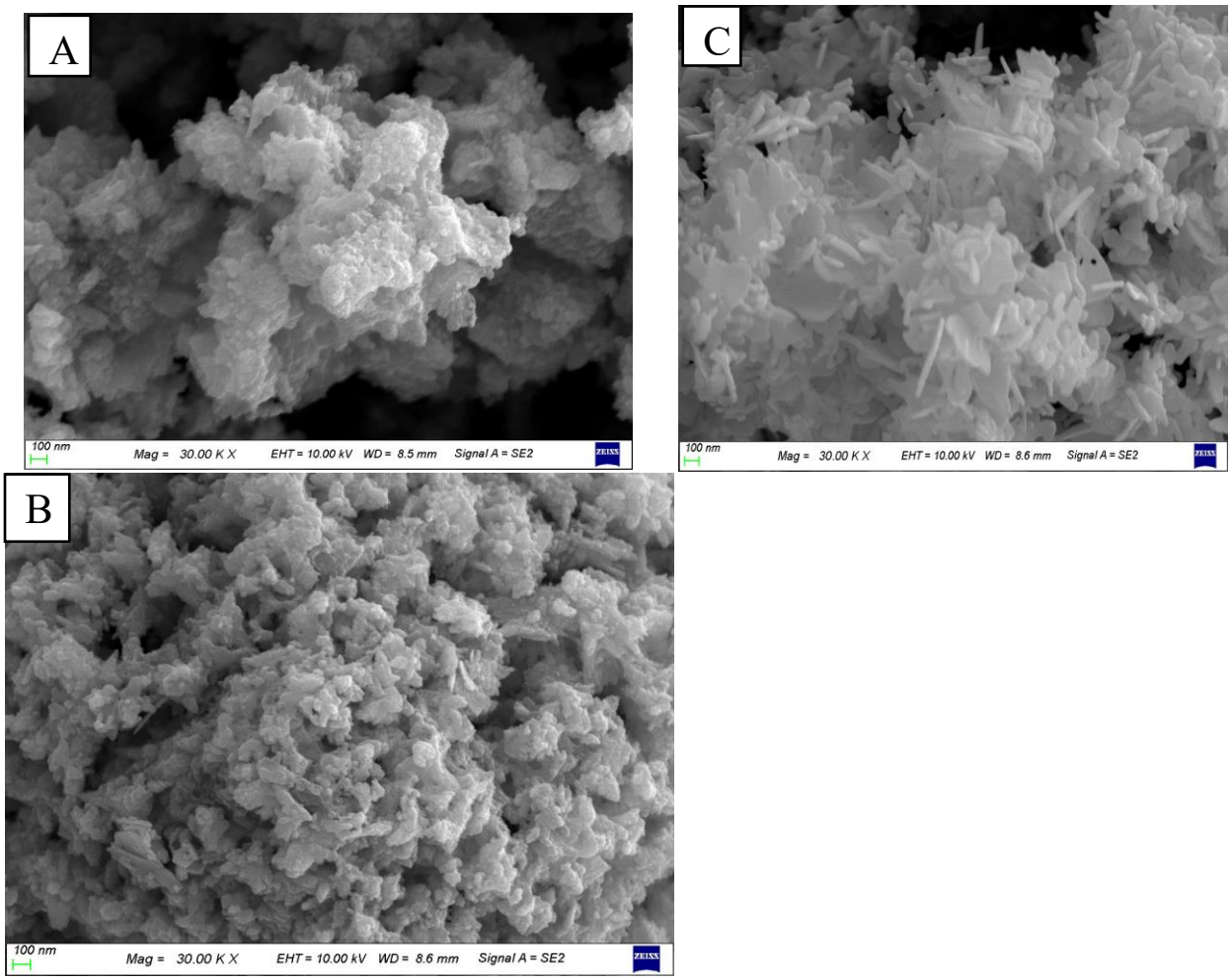

Figure 12 SEM images of ZnO NPs A (1:1), B (3:2), and C (2:3) ratios.

4.3. Antimicrobial Activity Test of ZnO NPs

4.3.1. Antibacterial activity test of ZnO NPs

To evaluate the antibacterial properties of the green synthesized ZnO NPs, different concentrations of the sample (50, 75, and 100 µg/mL) were tested against four bacterial gram-positive (*Staphylococcus aureus* and *Streptococcus pyogen*) and gram-negative (*Escherichia coli* and *Pseudomonas aeruginosa*) pathogens using an agar well diffusion procedure. The positive control of Amoxicillin against all the pathogens and the zone of inhibition values were measured as shown in Figure 13 and the results given in Table 4 from the table, indicate that the synthesized ZnO NPs have shown considerable antibacterial activity for all the four pathogens studied.

The difference in antibacterial activity is due to their difference in membrane structure (Gram-positive and Gram-negative). The gram-positive (*Staphylococcus aureus* and *Streptococcus*

pyogen) bacteria have a thick peptidoglycan layer and lack of outer membrane, whereas, the peptidoglycan layer in the *Escherichia coli*, *Pseudomonas aeruginosa* (Gram-negative) bacteria is thinner but surrounded by a lipid layer outside and have an outer membrane (Sundaraselvan & Darlin Quine, 2017)

In the antibacterial activity, initially, ZnO NPs attach to the surface of the bacterial cell membrane and then penetrate the bacteria. After penetration, they inactivate the enzymes of the microbes, generating hydrogen peroxide. Hence bacterial cells were dead (Sundaraselvan & Darlin Quine, 2017). Most kinds of the literature revealed that gram-negative bacteria were more sensitive to ZnO NPs treatments than gram-positive bacteria, and this could be attributed to the presence of a thick layer in the cell walls (peptidoglycan) of the latter group (Umar et al., 2019), but this is not always true. In this study, results revealed that gram-positive bacteria were more sensitive to ZnO NPs. This is because they tend to be more resistant to drying due to their thicker cell wall, but more susceptible to cleaning agents due to the lack of an outer membrane. However, gram-positive organisms that form spores are highly resistant to both drying and cleaning agents. Umar et al. also found a strong antibacterial potential against gram-positive bacteria using ZnO NPs synthesized from *Albizia lebbeck* stem bark (Umar et al., 2019), and concluded that the slight resistance of gram-negative bacteria is due to the presence of an outer membrane in their cell wall, which is similar to the results achieved in this work.

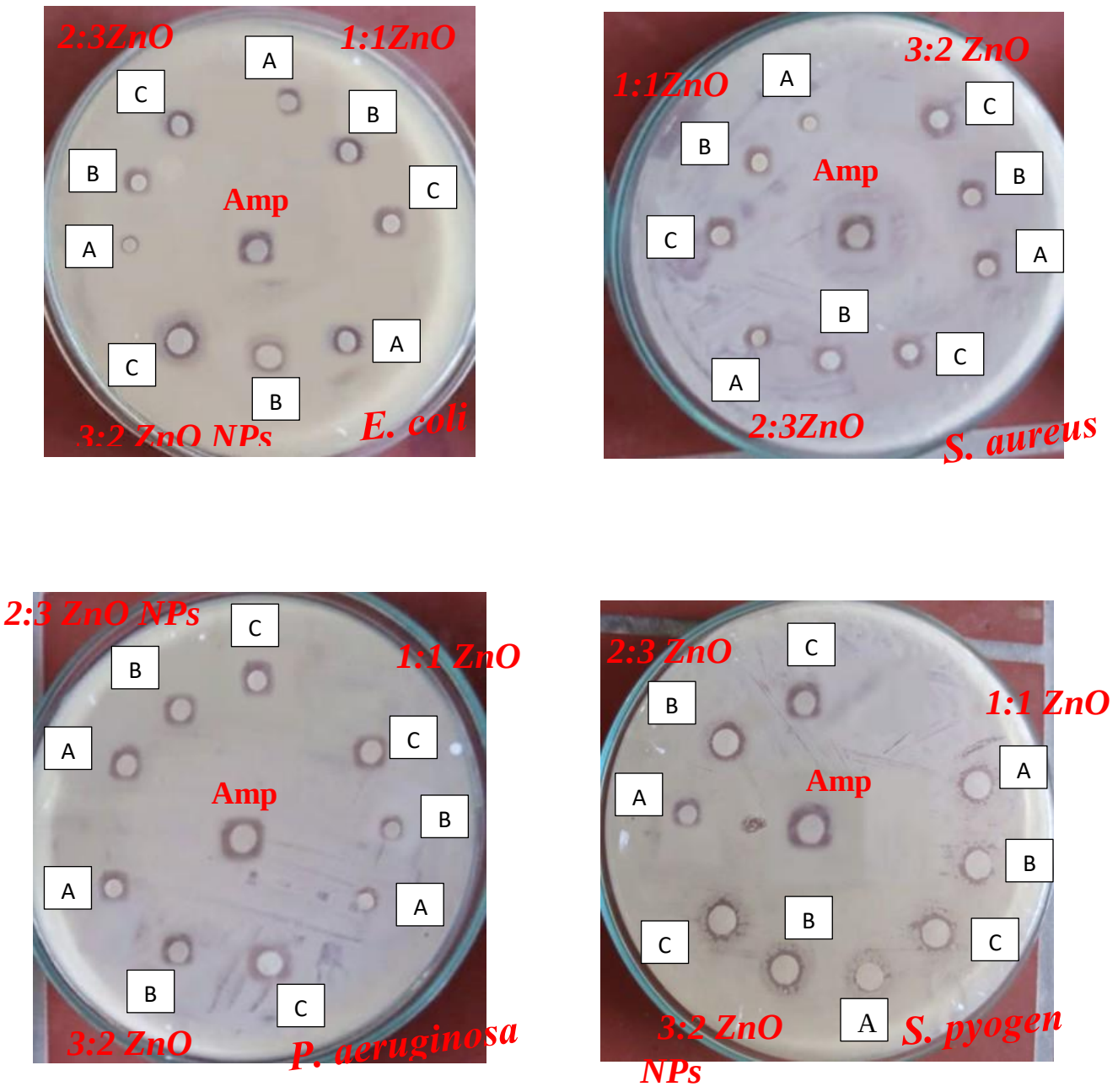

Figure 13 Antibacterial activity of synthesized ZnO NPs against bacterial pathogens, A, B, and C represent 50, 75, and 100 µg/mL respectively.

Table 4 Zone of inhibition (mm) of ZnO NPs against gram-positive and gram-negative bacteria pathogens.

Cpd & Conc. (ZnO NPs)		Bacteria strains and Zone of Inhibition in mm			
		E.coli ATCC25922	*S.aureus* ATCC25923	*P.aeruginosa* ATCC27853	*S.pyogen* ATCC19615
3:2 ZnO NPs	A= 50 µg/mL	8	9	8	9
	B= 75 µg/mL	10	10.5	9.5	10
	C= 100 µg/mL	12	12	11	11.5
2:3 ZnO NPs	A= 50 µg/mL	6	7	6	7
	B= 75 µg/mL	8	9	8	8
	C= 100 µg/mL	9	10	9	8.5
1:1 ZnO NPs	A= 50 µg/mL	7	8	7	8
	B= 75 µg/mL	9	9	9	9
	C= 100 µg/mL	11	10.5	10	10.5
	Amoxicillin (Amp)	13	13	12	13

From the results in Table 4, it was observed that ZnO NPs synthesized from *Coriandrum sativum* were sensitive to both gram-negative and gram-positive bacteria pathogens. According to Table 4, ZnO NPs for a 1:1 ratio at a high concentration of 100 µg/mL have a zone of inhibition of 10.5 mm for both gram-positive bacteria (*S. aureus* and *S. pyogen*) and gram-negative bacteria 11 mm and 10 mm (*E. coli* and *P. aeruginosa*) respectively, at 75 µg/mL both bacteria strains has recorded the same inhibition zone 9 mm, and at 50 µg/mL has a zone of inhibition 7 mm for both gram-negative bacteria (*E. coli* and *P. aeruginosa*) and 8 mm for both gram-positive bacteria (*S. aureus* and *S. pyogen*).

ZnO NPs for 2:3 ratio at 100, 75, and 50 µg/mL concentration have the zone of inhibition of 9, 8, and 6 mm respectively for both gram-negative bacteria (*E. coli* and *P. aeruginosa*), for both gram-positive bacteria (*S. aureus* and *S. pyogen*) at 100 µg/mL concentration has the zone of inhibition 10 and 8.5 mm and at 75 µg/mL 9 and 8 mm respectively, and also at 50 µg/mL concentration has a zone of inhibition 7mm. The lowest activity was determined with a low concentration of 50

µg/mL against both gram-negative bacteria (*E. coli* and *P. aeruginosa*) at 6 mm followed by gram-positive bacteria (*S. aureus* and *S. pyogen*) at 7 mm with ZnO NPs 1:1 and 2:3 with 50 µg/mL concentration.

For ZnO NPs 3:2 ratio the largest zones of inhibition were recorded with 100 µg/mL concentration against gram-positive (S. aureus) and gram-negative (*E.coli*) 12 mm and followed gram-positive (*S. pyogen*) 11.5 mm. at 75 µg/mL concentration has a zone of inhibition 10.5 and 10 mm for both gram-positive bacteria (*S. aureus* and *S. pyogen*) and gram-negative bacteria 10 mm and 9 mm (E. coli and P. aeruginosa) respectively, and at 50 µg/mL has a zone of inhibition 8 mm for both gram-negative bacteria (*E. coli* and *P. aeruginosa*) and 9 mm for both gram-positive bacteria (*S. aureus* and *S. pyogen*).

The antibacterial activity depends on the concentration and the crystalline structure of ZnO NPs. Increased cell death is achieved by increasing ZnO concentrations, which disrupt mitochondrial function, stimulating lactate dehydrogenase leakage and changing the morphology of the cell at concentrations of 50 to 100 µg/mL (Sirelkhatim et al., 2015). Sirelkhatim et al found that the higher concentration and the larger surface area can obtain better antibacterial activity and antibacterial activity also depended on the size, and it was probably due to the internalization and subsequent accumulation of NPs inside the cells until the particles reached the cytoplasmic region (Sirelkhatim et al., 2015). As the size of ZnO NP increases the antibacterial activities of ZnO nanoparticles slightly decrease. This is due to the surface area to volume ratio. As the surface area to volume ratio increases the size of ZnO NP decreases. From Table 4, ZnO (3:2) ratio nanoparticle had good inhibitory which means its highest antibacterial activities compared with other ratios.

4.3.2. Antifungal activities of ZnO NPs

The antifungal activities of synthesized ZnO NPs were evaluated for their antifungal effects against two human pathogenic fungal strains *C. Albicans* and *A. niger*. The antifungal test was performed using the agar disc diffusion method in the same manner as the standard protocol used similarly as previously used by researchers (Miri et al., 2019). The results obtained in this study revealed that all the studied ZnO NPs presented antifungal activity except 1:1 ZnO NPs at *Candida albicans* pathogen because of its lower concentration (15 mg/mL). The antifungal activities in terms of zone of inhibition in (mm) were measured for the three ratios (1:1, 2:3, and 3:2) of ZnO NPs against selected strains and compared to the standard as shown in Table 5 and Figure 14. The 3:2 ZnO

NPs had good inhibitory activity against both fungal strains. At 2:3 and 1:1 ZnO NPs at lower concentrations (15 mg/mL) did not have any activity since all the inhibition zones had less than 6 mm which is the same value that was the diameter of the disc.

The more plant leaf and low salt precursor nanoparticles designated as 3:2 ratio ZnO NPs were shows very good inhibitory zone with (14.83 ± 0.46, 13, and 10.66 ± 0.76 mm) against *C. albicans* at 25, 20, and 15mg/mL concentration and (16.16 ± 0.28, 14.83 ± 0.28, and 13.16 ± 0.28 mm) against *A. niger* with the same concentration which is the promising result which is comparable to standard Ketoconazole 20 for *C. albicans* and 19 for *A. niger*. In the same manner, the 1:1 ZnO NPs showed good inhibitory effects against selected fungal strains with an inhibition zone of (9.5 ± 0.43, 6.66 ± 0.20, and 0 mm) against *C. albicans* and (13.33 ± 0.28, 11.16 ± 0.28, and 9 mm) for *A. niger* at a concentration of 25, 20, and 15 mg/mL respectively.

The 2:3 ZnO NPs were shows intermediate inhibitory effects against selected fungal strains with an inhibition zone of (12.5 ± 0.5, 8.7 ± 0.65, and 5.1 ± 0.55 mm) against *C. albicans* and (11.2 ± 0.72, 7.3 ± 1.08, and 1.88 ± 3.17 mm) for *A. niger* at a concentration of 25, 20, and 15 mg/mL respectively.

The antifungal activities of the synthesized 3:2 ZnO NPs mostly target specific components of the fungal plasma membrane or its synthesis machinery or cell wall components of fungal cells are reasonably successful in combating fungal infections. The synergy among different phytochemicals especially in *Coriandrum sativum* leaves is being also projected on its effect against selected fungal strains.

Table 5. Zone of inhibition of synthesized ZnO NPs on the selected fungal strains

ZnO NPs Conc. (mg/mL)		Zone of inhibition in millimeter(mm)			
		Candida albicans		*Aspergillus niger*	
		Mean ±SD	*Ketoconazole* (positive control)	Mean ±SD	*Ketoconazole* (positive control)
3:2 ZnO NPs	25	14.83 ± 0.46	20	16.16 ± 0.28	19.5
	20	13		14.83 ± 0.28	
	15	10.66 ± 0.76		13.16 ± 0.28	
2:3 ZnO NPs	25	12.5 ± 0.5	18.5	11.2 ± 0.72	19
	20	8.7 ± 0.65		7.3 ± 1.08	
	15	5.1 ± 0.55		1.88 ± 3.17	
1:1 ZnO NPs	25	9.5 ± 0.43	15	13.33 ± 0.28	16
	20	6.66 ± 0.20		11.16 ± 0.28	
	15	0		9	

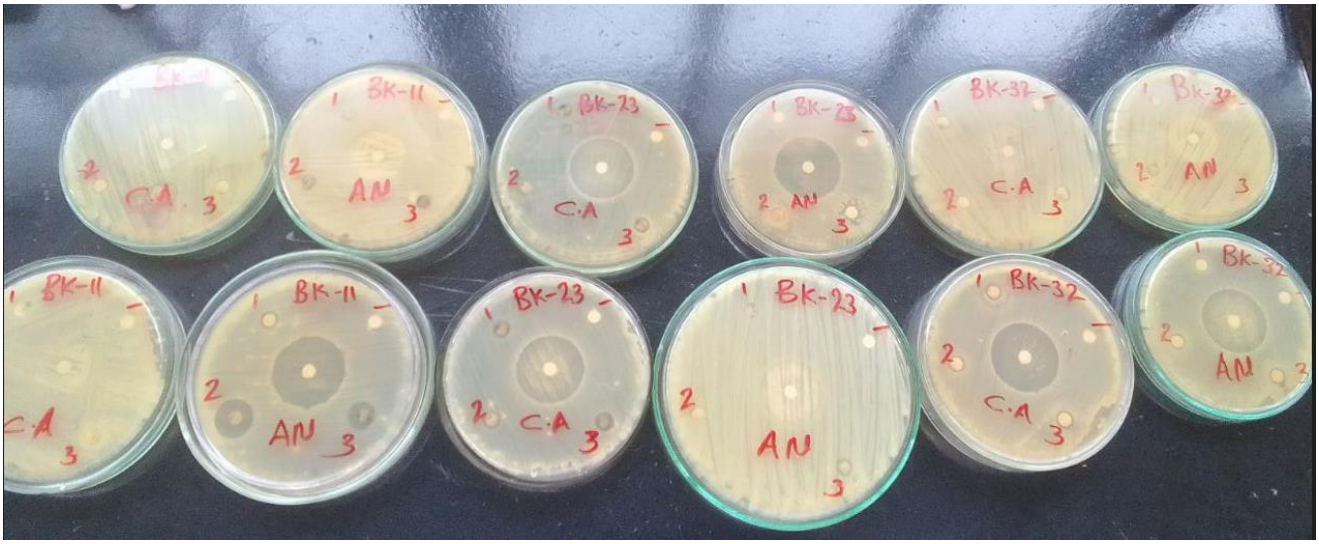

Figure 14 Antifungal activity of Synthesized ZnO NPs against selected fungal strains BK-11, BK-23, BK-32, AN, and C.A represents ZnO NPs 1:1, 2:3, and 3:2 ratios, *Aspergillus niger and Candida albicans* respectively.

4.3.3. Antioxidant activities of ZnO NPs

The antioxidant activity of the green synthesized ZnO NPs was measured by DPPH assay. An imbalance between antioxidants and ROS leads to oxidative stress and results in cellular damage. An important application of the NPs is their use as antioxidants and free radical scavenging (Elswaifi et al., 2012) to protect cells against the damaging effects of ROS. The Radical Scavenging Activity (RSA) of the three different ratios of ZnO NPs biosynthesized using *Coriandrum sativum* leaf and hexahydrate zinc nitrate precursor was examined in DPPH Assay using the percent of radicals scavenging assays shown in Table 6. Scavenging assay of the stable DPPH is widely used to study the radical scavenging property of materials. DPPH scavenging assay is the most popular method of studying antioxidant activity.

From Table 6 and Figure 15 the three ratios of ZnO NPs and the positive control ascorbic acid the concentration increases from 50 to 800 μg /mL the absorbance decreases. For the 1:1 ZnO NPs ratio, the concentration is at 50. 100, 200, 400, and 800 μg /mL the absorbance result was 1.069, 1.03, 1.016, 0.96, and 0.507 respectively. For the 2:3 ZnO NPs ratio, the concentration is at 50. 100, 200, 400, and 800 μg /mL the absorbance result was 1.013, 0.96, 0.891, 0.856, and 0.673 respectively. For the 3:2 ZnO NPs ratio, the concentration is at 50. 100, 200, 400, and 800 μg /mL the absorbance result was 0.884, 0.873, 0.837, 0.81, and 0.751 respectively, and although for the positive control ascorbic acid the concentration at 50. 100, 200, 400, and 800 μg /mL the absorbance result was 0.135, 0.121, 0.073, 0.037, and 0.024 respectively.

Table 6 The percent radical scavenging activity value from the DPPH assay of ZnO NPs ratios and ascorbic acid.

CONC	CONTROL	RATIOS						POSITIVE CONTROL	
	DPPH	1:1 ZnO NPs		2:3 ZnO NPs		3:2 ZnO NPs		Ascorbic Acid	
	Abs	Abs	%RSA	Abs	%RSA	Abs	%RSA	Abs	%RSA
	1.099	0.507	53.867	0.673	38.762	0.751	31.665	0.024	97.816
800	1.099	0.96	12.648	0.856	22.111	0.81	26.297	0.037	96.633
400	1.099	1.016	7.552	0.891	18.926	0.837	23.840	0.073	93.358
200	1.099	1.03	6.278	0.96	12.648	0.873	20.564	0.121	88.99
100	1.099	1.069	2.73	1.013	7.825	0.884	19.563	0.135	87.72

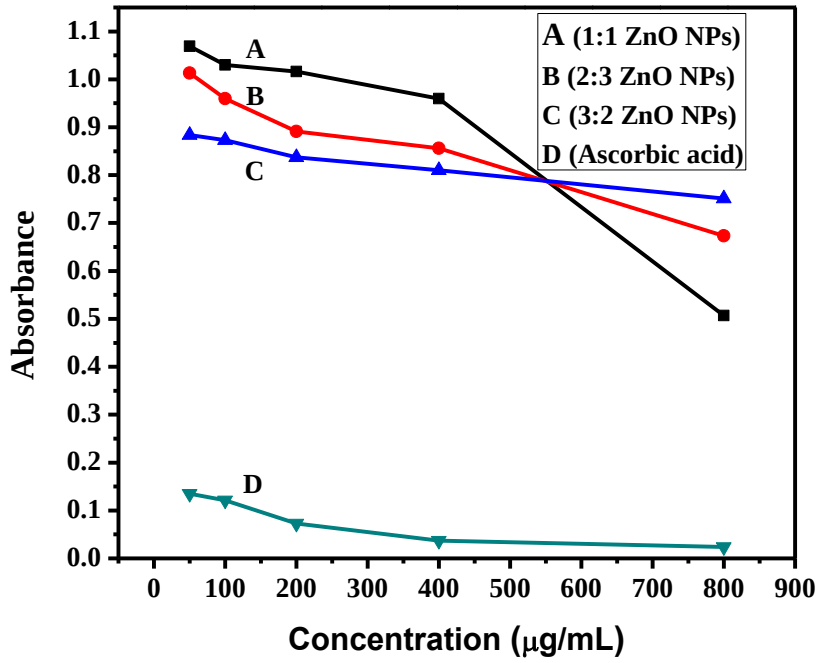

Figure 15 In the DPPH assay of ZnO NPs ratios and ascorbic acid concentration *versus* absorbance graph.

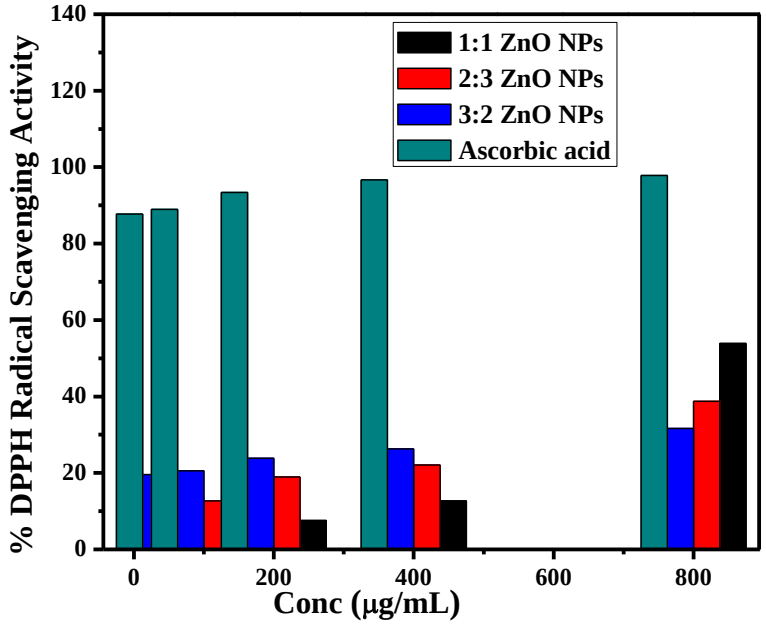

Figure 16 DPPH assay of the synthesized ZnO NPs antioxidant activity at 50, 100, 200, 400, and 800 µg /mL concentration.

From Table 6 the result of three ratios of ZnO NPs and one positive control ascorbic acid shows at the lower the absorbance value the higher the antioxidant activity of the percent radical scavenging activity (% RSA). The concentration of the sample increases the percent of inhibition of radical scavenging activity was also increases shown in Figure 16 and Table 6. From Table 6, the green synthesized ZnO NPs ratios and ascorbic acid as the concentration increase from 50 to 800 μg /mL, the % RSA also increases. Result for 1:1 ZnO NPs ratio at concentrations 50, 100, 200, 400, and 800 μg /mL the percent inhibition of radical scavenging activity was 2.73, 6.278, 7.552, 12.648, and 53.867 respectively. For 2:3 ZnO NPs ratio at concentration 50, 100, 200, 400, and 800 μg /mL the percent inhibition of radical scavenging activity was 7.825, 12.648, 18.926, 22.111, and, 38.762 respectively although for 3:2 ZnO NPs ratio at concentration 50, 100, 200, 400, and 800 μg /mL the percent inhibition of radical scavenging activity was 19.563, 20.563, 23.840, 26.297, and 31.665 respectively and for ascorbic acid at concentration 50, 100, 200, 400, and 800 μg /mL the percent inhibition of radical scavenging activity was 87.72, 88.99, 93.358, 96.633, and 97.816 respectively.

The value of the 1:1 ratio of ZnO NPs at 800 μg/mL concentration showed nearly good efficacy as compared to the standard ascorbic acid. The 3:2 ratio of ZnO NPs was at all the concentrations it showed antioxidant activity but compared with the positive control ascorbic acid its activity was lower.

5. CONCLUSIONS AND RECOMMENDATIONS

5.1. Conclusions

In this study, hexahydrate zinc nitrate was used as a precursor and *Coriandrum sativum* leaf extract as a capping and stabilizing agent to create ZnO nanoparticles. Thermal stability of biosynthesized ZnO NPs was demonstrated by TGA study over 466 °C. XRD and FTIR were used to determine the size, crystallinity, and functional group of the nanoparticles. The creation of pure Wurtzite structure in ZnO NPs was shown by the XRD pattern. The 3:2 ratio ZnO NPs which were capped and stabilized leaf extract were found to be lesser in size. The SEM images confirmed the formation of hexagonal particles and UV-vis absorption peak at wave length 319.84 nm and the band gap energy of 3.17 eV confirmed the formation of ZnO NPs. Moreover, the *Coriandrum sativum* leaf extract stabilized ZnO NPs exhibited considerable antimicrobial activity against pathogenic bacteria and fungi which is comparable with that of standard antibiotics. Based on these results I conclude that the synthesized ZnO NPs with a 3:2 ratio showed significant antimicrobial activities than the other ratios because it has a smaller size than the other ratios. Gram-positive bacteria have more sensitive to ZnO NPs than gram-negative bacteria. Compared with Gram-positive bacteria, Gram-negative bacteria are most resistant to ZnO NPs. The DPPH assay of the synthesized ZnO NPs indicated ZnO NPs have antioxidant activity.

5.2. Recommendation

ZnO nanoparticle synthesis through green methods by using *Coriandrum sativum* leaf is one of the emerging research areas with huge future prospective. Thus, further studies may be required for the synthesis of zinc oxide nanoparticles characterized using different instruments TEM (transmission electron microscopy), HRTEM (high-resolution transmission electron microscopy), SEM-EDS (scanning electron microscopy-Energy dispersive spectroscopy), and applications such as in the field of photocatalytic activity in the removal of heavy metals, and dye, electrochemical, and biomedical applications.

6. REFERENCE

Agarwal, H., Venkat Kumar, S., & Rajeshkumar, S. (2017). A review on green synthesis of zinc oxide nanoparticles – An eco-friendly approach. *Resource-Efficient Technologies*, *3*(4), 406–413. https://doi.org/10.1016/j.reffit.2017.03.002

Ajitha, B., Kumar Reddy, Y. A., Reddy, P. S., Jeon, H. J., & Ahn, C. W. (2016). Role of capping agents in controlling silver nanoparticles size, antibacterial activity and potential application as optical hydrogen peroxide sensor. *RSC Advances*, *6*(42), 36171–36179. https://doi.org/10.1039/c6ra03766f

Akintelu, S. A., & Folorunso, A. S. (2020). A Review on Green Synthesis of Zinc Oxide Nanoparticles Using Plant Extracts and Its Biomedical Applications. *BioNanoScience*, *10*(4), 848–863. https://doi.org/10.1007/s12668-020-00774-6

Altemimi, A., Lakhssassi, N., Baharlouei, A., Watson, D. G., & Lightfoot, D. A. (2017). Phytochemicals: Extraction, isolation, and identification of bioactive compounds from plant extracts. *Plants*, *6*(4). https://doi.org/10.3390/plants6040042

Asgarpanah, J. (2012). Phytochemistry, pharmacology and medicinal properties of Coriandrum sativum L. *African Journal of Pharmacy and Pharmacology*, *6*(31), 2340–2345. https://doi.org/10.5897/ajpp12.901

Ashika, B. ., Roy, C. L., S, N., S, S. K., Suma, A., & Sathyamurthy, B. (2018). Phytochemical Studies on the Methanolic Extract of Coriander Sativum Leaves - An In Vitro Approach. *European of Biomedical and Pharmaceutical Sciences*, *5*(8), 494–500. http://www.ejbps.com

Balantrapu, K., & Goia, D. V. (2009). Silver nanoparticles for printable electronics and biological applications. *Journal of Materials Research*, *24*(9), 2828–2836. https://doi.org/10.1557/jmr.2009.0336

Balcha, A., Yadav, O. P., & Dey, T. (2016). Photocatalytic degradation of methylene blue dye by zinc oxide nanoparticles obtained from precipitation and sol-gel methods. *Environmental Science and Pollution Research*, *23*(24), 25485–25493. https://doi.org/10.1007/s11356-016-7750-6

Basnet, P., Inakhunbi Chanu, T., Samanta, D., & Chatterjee, S. (2018). A review on bio-synthesized zinc oxide nanoparticles using plant extracts as reductants and stabilizing agents. *Journal of Photochemistry and Photobiology B: Biology*, *183*, 201–221. https://doi.org/10.1016/j.jphotobiol.2018.04.036

Bhuiyan, M. N. I., Begum, J., & Sultana, M. (2009). Chemical composition of leaf and seed essential oil of Coriandrum sativum L. from Bangladesh. *Bangladesh Journal of Pharmacology*, *4*(2), 150–153. https://doi.org/10.3329/bjp.v4i2.2800

Biswas, B., Rogers, K., McLaughlin, F., Daniels, D., & Yadav, A. (2013). Antimicrobial activities of leaf extracts of guava (psidium guajava L.) on two gram-negative and gram-positive bacteria. *International Journal of Microbiology*, *2013*. https://doi.org/10.1155/2013/746165

Blondeau, D., Roy, L., Dumont, S., Godin, G., & Martineau, I. (2005). Physicians' and pharmacists' attitudes toward the use of sedation at the end of life: Influence of prognosis and type of suffering. *Journal of Palliative Care*, *21*(4), 238–245. https://doi.org/10.1177/082585970502100402

Cruz, D. M., Mostafavi, E., Vernet-Crua, A., Barabadi, H., Shah, V., Cholula-Díaz, J. L., Guisbiers, G., & Webster, T. J. (2020). Green nanotechnology-based zinc oxide (ZnO) nanomaterials for biomedical applications: A review. *JPhys Materials*, *3*(3). https://doi.org/10.1088/2515-7639/ab8186

Dadi, R., Azouani, R., Traore, M., Mielcarek, C., & Kanaev, A. (2019). Antibacterial activity of ZnO and CuO nanoparticles against gram positive and gram negative strains. *Materials Science and Engineering C*, *104*, 109968. https://doi.org/10.1016/j.msec.2019.109968

Darvishi, E., Kahrizi, D., & Arkan, E. (2019). Comparison of different properties of zinc oxide nanoparticles synthesized by the green (using Juglans regia L. leaf extract) and chemical methods. *Journal of Molecular Liquids*, *286*. https://doi.org/10.1016/j.molliq.2019.04.108

Das, D., Nath, B. C., Phukon, P., kalita, A., & Dolui, S. K. (2013). Synthesis of ZnO nanoparticles and evaluation of antioxidant and cytotoxic activity. *Colloids and Surfaces B: Biointerfaces*, *111*, 556–560. https://doi.org/10.1016/j.colsurfb.2013.06.041

Degefa, A., Bekele, B., Jule, L. T., Fikadu, B., Ramaswamy, S., Dwarampudi, L. P., Nagaprasad,

N., & Ramaswamy, K. (2021). Green Synthesis, Characterization of Zinc Oxide Nanoparticles, and Examination of Properties for Dye-Sensitive Solar Cells Using Various Vegetable Extracts. *Journal of Nanomaterials*, *2021*. https://doi.org/10.1155/2021/3941923

Demissie, M. G., Sabir, F. K., Edossa, G. D., & Gonfa, B. A. (2020). Synthesis of Zinc Oxide Nanoparticles Using Leaf Extract of Lippia adoensis (Koseret) and Evaluation of Its Antibacterial Activity. *Journal of Chemistry*, *2020*. https://doi.org/10.1155/2020/7459042

Doan Thi, T. U., Nguyen, T. T., Thi, Y. D., Ta Thi, K. H., Phan, B. T., & Pham, K. N. (2020). Green synthesis of ZnO nanoparticles using orange fruit peel extract for antibacterial activities. *RSC Advances*, *10*(40), 23899–23907. https://doi.org/10.1039/d0ra04926c

Ealias, A. M., & Saravanakumar, M. P. (2017). A review on the classification, characterisation, synthesis of nanoparticles and their application. *IOP Conference Series: Materials Science and Engineering*, *263*(3). https://doi.org/10.1088/1757-899X/263/3/032019

Elswaifi, S., Palmieri, J., Hockey, K., & Rzigalinski, B. (2012). Antioxidant Nanoparticles for Control of Infectious Disease. *Infectious Disorders - Drug Targets*, *9*(4), 445–452. https://doi.org/10.2174/187152609788922528

Espinosa, H. D., Bernal, R. A., & Minary-Jolandan, M. (2012). A review of mechanical and electromechanical properties of piezoelectric nanowires. *Advanced Materials*, *24*(34), 4656–4675. https://doi.org/10.1002/adma.201104810

Gharagozloo, M., Kalantari, H., Rezaei, A., Maracy, M. R., Salehi, M., Bahador, A., Hassannejad, N., Narimani, M., Sanei, M. H., Bayat, B., & Ghazanfari, H. (2015). CLINICAL STUDY Immune-mediated cochleovestibular disease. *Bratislavsk?? Lek??Rske Listy*, *116*(5), 296–301. https://doi.org/10.4149/BLL

Gharpure, S., & Ankamwar, B. (2020). Synthesis and Antimicrobial Properties of Zinc Oxide Nanoparticles. *Journal of Nanoscience and Nanotechnology*, *20*(10), 5977–5996. https://doi.org/10.1166/jnn.2020.18707

Haque, M. J., Bellah, M. M., Hassan, M. R., & Rahman, S. (2020). Synthesis of ZnO nanoparticles by two different methods & comparison of their structural, antibacterial, photocatalytic and optical properties. *Nano Express*, *1*(1). https://doi.org/10.1088/2632-959X/ab7a43

Hassan, A. A., Howayda, M. E., & Mahmoud, H. H. (2013). *Effect of Zinc Oxide Nanoparticles on the Growth of Mycotoxigenic Mould*. *May 2013*.

Hossain, A., Abdallah, Y., Ali, M. A., Masum, M. M. I., Li, B., Sun, G., Meng, Y., Wang, Y., & An, Q. (2019). Lemon-fruit-based green synthesis of zinc oxide nanoparticles and titanium dioxide nanoparticles against soft rot bacterial pathogen dickeya dadantii. *Biomolecules*, *9*(12), 1–15. https://doi.org/10.3390/biom9120863

Hudzicki, J. (2012). Kirby-Bauer Disk Diffusion Susceptibility Test Protocol Author Information. *American Society For Microbiology*, *December 2009*, 1–13. https://www.asm.org/Protocols/Kirby-Bauer-Disk-Diffusion-Susceptibility-Test-Pro

Hussein, M. Z., Azmin, W. H. W. N., Mustafa, M., & Yahaya, A. H. (2009). Bacillus cereus as a biotemplating agent for the synthesis of zinc oxide with raspberry- and plate-like structures. *Journal of Inorganic Biochemistry*, *103*(8), 1145–1150. https://doi.org/10.1016/j.jinorgbio.2009.05.016

Joudeh, N., & Linke, D. (2022). Nanoparticle classification , physicochemical properties , characterization , and applications : a comprehensive review for biologists. *Journal of Nanobiotechnology*, 1–29. https://doi.org/10.1186/s12951-022-01477-8

Jubeh, B., Breijyeh, Z., & Karaman, R. (2020). Resistance of gram-positive bacteria to current antibacterial agents and overcoming approaches. *Molecules*, *25*(12). https://doi.org/10.3390/molecules25122888

Kalpana, V. N., & Devi Rajeswari, V. (2018). A Review on Green Synthesis, Biomedical Applications, and Toxicity Studies of ZnO NPs. *Bioinorganic Chemistry and Applications*, *2018*. https://doi.org/10.1155/2018/3569758

Kassahun, B. M. (2018). *Performance of Ethiopian Coriander (Coriandrum sativum L) Accessions in Vegetative , Phenological , Generative and Chemical Characters*. *January*.

Khalfa, E. F., Nafaee, Z. H., Abdullah, F. N., Bdair, G. S., Niema, R. M., Salman, H. D., & Hussein, F. H. (2019). Synthesis and characterizations of zinc oxide nanoparticles-loaded chloramphenicol for antibacterial applications. *Annals of Tropical Medicine and Public Health*, *22*(12). https://doi.org/10.36295/ASRO.2019.221217

Kolodziejczak-Radzimska, A., & Jesionowski, T. (2014). Zinc oxide-from synthesis to application: A review. *Materials*, *7*(4), 2833–2881. https://doi.org/10.3390/ma7042833

Kumar, P., & Walia, Y. K. (2015). *Synthesis and Structural properties of Zinc Oxide Nano Particles (ZnO NPs): A Review Synthesis and Structural properties of Zinc Oxide Nano Particles (ZnO NPs): A Review Pankaj Kumar and Yogesh Kumar Walia*. *May 2014*.

Lakshmi, S. J., Bai R S, R., H, S., & Nidoni, U. kumar. (2017). a Review Study of Zinc Oxide Nanoparticles Synthesis From Plant Extracts. *Green Chemistry & Technology Letters*, *3*(2), 26–37. https://doi.org/10.18510/gctl.2017.321

Laribi, B., Kouki, K., Hamdi, M. M., & Bettaieb, T. (2015). PT. *Fitoterapia*. https://doi.org/10.1016/j.fitote.2015.03.012

Liewhiran, C., & Phanichphant, S. (2007). Improvement of flame-made ZnO nanoparticulate thick film morphology for ethanol sensing. *Sensors*, *7*(5), 650–675. https://doi.org/10.3390/s7050650

Lu, P. J., Huang, S. C., Chen, Y. P., Chiueh, L. C., & Shih, D. Y. C. (2015). Analysis of titanium dioxide and zinc oxide nanoparticles in cosmetics. *Journal of Food and Drug Analysis*, *23*(3), 587–594. https://doi.org/10.1016/j.jfda.2015.02.009

Mandal, S., & Mandal, M. (2015). Coriander (Coriandrum sativum L.) essential oil: Chemistry and biological activity. *Asian Pacific Journal of Tropical Biomedicine*, *5*(6), 421–428. https://doi.org/10.1016/j.apjtb.2015.04.001

Miri, A., Ebrahimy, O., Khatami, M., & Sarani, M. (2019). *Materials Science & Engineering C Zinc oxide nanoparticles : Biosynthesis , characterization , antifungal and cytotoxic activity*. *104*(June). https://doi.org/10.1016/j.msec.2019.109981

Parihar, V., Raja, M., & Paulose, R. (2018). A brief review of structural, electrical and electrochemical properties of zinc oxide nanoparticles. *Reviews on Advanced Materials Science*, *53*(2), 119–130. https://doi.org/10.1515/rams-2018-0009

Peter, J. K., Kumar, Y., Pandey, P., & Masih, H. (2014). Antibacterial Activity of Seed and Leaf Extract of Carica Papaya var. Pusa dwarf Linn. *IOSR Journal of Pharmacy and Biological Sciences*, *9*(2), 29–37. https://doi.org/10.9790/3008-09272937

Ranganatha, V. L., Nithin, K. S., Khanum, S. A., Nagaraju, G., & Mallikarjunaswamy, C. (2019). Zinc oxide nanoparticles: A significant review on synthetic strategies, characterization and applications. *AIP Conference Proceedings*, *2162*(October). https://doi.org/10.1063/1.5130299

Sabir, S., Arshad, M., & Chaudhari, S. K. (2014). Zinc oxide nanoparticles for revolutionizing agriculture: Synthesis and applications. *Scientific World Journal*, *2014*. https://doi.org/10.1155/2014/925494

Safawo, T., Sandeep, B. V, Pola, S., & Tadesse, A. (2018). OpenNano Synthesis and characterization of zinc oxide nanoparticles using tuber extract of anchote (Coccinia abyssinica (Lam .) Cong .) for antimicrobial and antioxidant activity assessment. *OpenNano*, *3*(August), 56–63. https://doi.org/10.1016/j.onano.2018.08.001

Savi, G. D., Bortoluzzi, A. J., & Scussel, V. M. (2013). Antifungal properties of Zinc-compounds against toxigenic fungi and mycotoxin. *International Journal of Food Science and Technology*, *48*(9), 1834–1840. https://doi.org/10.1111/ijfs.12158

Sharma, D., Rajput, J., Kaith, B. S., Kaur, M., & Sharma, S. (2010). Synthesis of ZnO nanoparticles and study of their antibacterial and antifungal properties. *Thin Solid Films*, *519*(3), 1224–1229. https://doi.org/10.1016/j.tsf.2010.08.073

Sharma, N., Jandaik, S., & Kumar, S. (2016). Synergistic activity of doped zinc oxide nanoparticles with antibiotics: Ciprofloxacin, ampicillin, fluconazole and amphotericin B against pathogenic microorganisms. *Anais Da Academia Brasileira de Ciencias*, *88*(3), 1689–1698. https://doi.org/10.1590/0001-3765201620150713

Shrivastava, D. K. (2017). PHYTOCHEMICAL ANALYSIS OF A MIRACLE HERB Coriander sativum. *Indian J.Sci.Res*, *13*(2), 9–14.

Siddiqi, K. S., ur Rahman, A., Tajuddin, & Husen, A. (2018). Properties of Zinc Oxide Nanoparticles and Their Activity Against Microbes. *Nanoscale Research Letters*, *13*. https://doi.org/10.1186/s11671-018-2532-3

Singh, J., Dutta, T., Kim, K. H., Rawat, M., Samddar, P., & Kumar, P. (2018). “Green” synthesis of metals and their oxide nanoparticles: Applications for environmental remediation. *Journal*

of Nanobiotechnology, *16*(1), 1–24. https://doi.org/10.1186/s12951-018-0408-4

Sirelkhatim, A., Mahmud, S., Seeni, A., Kaus, N. H. M., Ann, L. C., Bakhori, S. K. M., Hasan, H., & Mohamad, D. (2015). Review on zinc oxide nanoparticles: Antibacterial activity and toxicity mechanism. *Nano-Micro Letters*, *7*(3), 219–242. https://doi.org/10.1007/s40820-015-0040-x

Stanaszek-Tomal, E. (2020). Bacterial concrete as a sustainable building material? *Sustainability (Switzerland)*, *12*(2). https://doi.org/10.3390/su12020696

Sun, Q., Li, J., & Le, T. (2018). Zinc Oxide Nanoparticle as a Novel Class of Antifungal Agents: Current Advances and Future Perspectives. *Journal of Agricultural and Food Chemistry*, *66*(43), 11209–11220. https://doi.org/10.1021/acs.jafc.8b03210

Sundaraselvan, G., & Darlin Quine, S. (2017). Green Synthesis of Zinc Oxide Nanoparticles using Seed Extract of Murraya koenigii and Their Antimicrobial Activity against Some Human Pathogens. *Journal of Nanoscience and Technology*, *3*(4), 289–292.

Suresh, J., Pradheesh, G., Alexramani, V., Sundrarajan, M., & Hong, S. I. (2018). Green synthesis and characterization of zinc oxide nanoparticle using insulin plant (Costus pictus D. Don) and investigation of its antimicrobial as well as anticancer activities. *Advances in Natural Sciences: Nanoscience and Nanotechnology*, *9*(1). https://doi.org/10.1088/2043-6254/aaa6f1

Tsukatani, T., Suenaga, H., Shiga, M., Noguchi, K., Ishiyama, M., Ezoe, T., & Matsumoto, K. (2012). Comparison of the WST-8 colorimetric method and the CLSI broth microdilution method for susceptibility testing against drug-resistant bacteria. *Journal of Microbiological Methods*, *90*(3), 160–166. https://doi.org/10.1016/j.mimet.2012.05.001

Umar, H., Kavaz, D., & Rizaner, N. (2019). Biosynthesis of zinc oxide nanoparticles using albizia lebbeck stem bark, and evaluation of its antimicrobial, antioxidant, and cytotoxic activities on human breast cancer cell lines. *International Journal of Nanomedicine*, *14*, 87–100. https://doi.org/10.2147/IJN.S186888

Vishwakarma, K., The, U., & Guidance, S. (2013). *USING Abrus precatorius SEEDS EXTRACT AND THEIR CHARACTERIZATION Thesis submitted to Department of life science for the partial fulfillment of the*. 41.

Xu, J., Huang, Y., Zhu, S., Abbes, N., Jing, X., & Zhang, L. (2021). A review of the green synthesis of ZnO nanoparticles using plant extracts and their prospects for application in antibacterial textiles. *Journal of Engineered Fibers and Fabrics*, *16*. https://doi.org/10.1177/15589250211046242

Zare, M., Namratha, K., Byrappa, K., Surendra, D. M., Yallappa, S., & Hungund, B. (2018). Surfactant assisted solvothermal synthesis of ZnO nanoparticles and study of their antimicrobial and antioxidant properties. *Journal of Materials Science and Technology*, *34*(6), 1035–1043. https://doi.org/10.1016/j.jmst.2017.09.014

Zhang, Z. Y., & Xiong, H. M. (2015). Photoluminescent ZnO nanoparticles and their biological applications. *Materials*, *8*(6), 3101–3127. https://doi.org/10.3390/ma8063101